# Anharmonic vibrational spectroscopy of Polycyclic Aromatic Hydrocarbons (PAHs)

Giacomo Mulas,[1,2] Cyril Falvo,[3,4] Patrick Cassam-Chenaï,[5] and Christine Joblin[1]
[1)] *IRAP, Université de Toulouse, CNRS, UPS, CNES, 9 Av. du Colonel Roche, 31028 Toulouse Cedex 4, France*
[2)] *Istituto Nazionale di Astrofisica (INAF), Osservatorio Astronomico di Cagliari, 09047 Selargius (CA), Italy*[a)]
[3)] *Institut des Sciences Moléculaires d'Orsay (ISMO), CNRS, Univ. Paris-Sud, Université Paris-Saclay, 91405 Orsay, France*
[4)] *Univ. Grenoble Alpes, CNRS, LIPhy, 38000 Grenoble, France*
[5)] *Université Côte d'Azur, CNRS, LJAD, UMR 7351, 06100 Nice, France*

This supplementary material contains:

- A description of the different ethylene oxide force fields that have been used for benchmarking purposes
- Table I: Comparison of the VMFCI reference calculation with HI-RRBPM calculation D of Ref. 1 for the force field adimensioned with DFT quadratic force constants
- Table II: Comparison of the VMFCI reference calculation with a previous VMFCI calculation using a different contraction-truncation scheme for the force field adimensioned with coupled-cluster quadratic force constants
- Table III: List of harmonic vibrational normal modes of pyrene.
- Table IV: List of harmonic vibrational normal modes of coronene
- Table V: List of (significantly IR-active) anharmonic states of pyrene as a function of $r$ values, for fixed $h = 8$
- Figures 1–27: Anharmonic spectra of pyrene and coronene

## I. VMFCI CALCULATIONS

### A. Different ethylene oxide force fields

The ethylene oxide quartic force field of Bégué *et al.*[2] has now become a classical benchmark for methods solving the anharmonic vibrational Schrödinger equation. However, there are three different versions of this force field:

1. The version provided as supplementary material of Ref. 2, which was actually only employed for the largest P-VMWCI calculation. It lacks one cubic and seven quartic force constants that were removed from the original DFT quartic force field. This was necessary to alleviate the computational effort required to perform the $\gamma = 3$ P-VMWCI calculation of Ref. 2.
2. The version used in the main text of present work and in the VMFCI calculations of Refs. 1 and 2. It is the combination of the CCSD(T)/cc-pVTZ quadratic constants and the full set of B3LYP/6-31+G(d,p) cubic and quartic force constants in mass-weighted, Cartesian, normal coordinates. In terms of adimensional coordinates, the force field obtained amounts to cubic and quartic force constants rescaled by using CCSD(T)/cc-pVTZ quadratic constants. It is this force field that has been used for benchmarking AnharmoniCaOs.
3. The version used in recent investigations.[1,3,4] It differs from the previous one by the fact that the cubic and quartic force constants were adimensioned by using the B3LYP/6-31+G(d,p) quadratic constants. This results in a noticeably different force field: for instance, the zero point energy with this force field differs by 2 $cm^{-1}$from that obtained with the previous force field, (compare the two tables below).

### B. Comparison of the new VMFCI reference calculation with HI-RRBPM results

Two fairly large numerical calculations of the 200 lowest eigenvalues of the vibrational Hamiltonian associated to force field 3 have appeared recently. One is based on the Adaptative Vibrational Configuration Interaction (A-VCI) algorithm,[4] and the other on the Hierarchical Intertwined Reduced-Rank Block Power Method (HI-RRBPM).[1] We postpone a discussion of the remarkable A-VCI results to a forthcoming publication. Here, we just validate a new Vibrational Mean Field Configuration Interaction (VMFCI) contraction-truncation scheme

[a)] Electronic mail: gmulas@oa-cagliari.inaf.it

against the latest HI-RRBPM calculation (calculation "D" of Ref. 1).

The new contraction-truncation scheme is the following:
- The calculation starts with the same modal basis set of 100 harmonic function on each of the 15 modes, then a VSCF calculation is converged to machine precision in seven VMFCI iterations. The common zero point energy (ZPE) of the 15 modes is then 12539.269841 $cm^{-1}$.
- Then, we make 6 contractions: the four C−H stretching modes $\nu_1 - \nu_6 - \nu_9 - \nu_{13}$, the two H−C−H scissoring modes $\nu_2 - \nu_{10}$, the three ring breathing and deformation modes $\nu_3 - \nu_5 - \nu_{12}$, the two wagging modes $\nu_4 - \nu_{11}$, the two twisting modes $\nu_7 - \nu_{14}$, the two rocking modes $\nu_8 - \nu_{15}$, with truncation thresholds on the sum of the energies of 34072 $cm^{-1}$ for the stretchings, 17000 $cm^{-1}$ for the ring deformations and 30000 $cm^{-1}$ for the four other contractions. This partition is iterated once and the 6 ZPE's decrease down to $12501.358 \pm 0.001$ $cm^{-1}$. All this is abbreviated by VSCFCI($\{\nu_1, \nu_6, \nu_9, \nu_{13}\}$, 34072; $\{\nu_2, \nu_{10}\}$, 30000; $\{\nu_3, \nu_5, \nu_{12}\}$, 17000; $\{\nu_4, \nu_{11}\}$, 30000; $\{\nu_7, \nu_{14}\}$ , 30000; $\{\nu_8, \nu_{15}\}$, 30000).
- Next, we make a coarser partition of only two contractions and play on both individual energy and sum of energy thresholds in a single VMFCI step:
VMFCI($\{\{\nu_1, \nu_6, \nu_9, \nu_{13}\}_{17523}, \{\nu_2, \nu_{10}\}_{12272}, \{\nu_8, \nu_{15}\}_{12077}\}$, 17914;
$\{\{\nu_3, \nu_5, \nu_{12}\}_{11459}, \{\nu_4, \nu_{11}\}_{11156}, \{\nu_7, \nu_{14}\}_{9633}\}$, 15280 ),
(the subscripts are the thresholds in $cm^{-1}$ on the individual energies of the component of the new contractions).
- Finally, the two previous contraction are contracted in a VCI step with a truncation threshold of 6367.5 $cm^{-1}$ on the second component and a threshold of 11956.6 $cm^{-1}$ on the sum of the component energies. The size of this VCI is 430769 basis functions, it splits into 4 $C_{2V}$-symmetry blocks of dimensions 108147 for A1, 107421 for A2, 107740 for B1, 107461 for B2.

The whole calculation is denoted VMFCI(11956.6) in the table below and the wave numbers are compared to those of calculation D of Ref. 1.

TABLE I: Lowest 200 vibrational energy levels (in $cm^{-1}$) of ethylene oxide for force field 3

| irreps. | VMFCI(11956.6) | Ref. 1 | Assignment[1] |
|---|---|---|---|
| $A_1$ | 12461.57 | 12461.65 | ZPE |
| $B_2$ | 792.80 | 793.10 | $\nu_{15}$ |
| $B_1$ | 821.98 | 822.00 | $\nu_{12}$ |
| $A_1$ | 878.32 | 878.33 | $\nu_5$ |
| $A_2$ | 1017.31 | 1017.49 | $\nu_8$ |
| $A_1$ | 1121.64 | 1121.94 | $\nu_4$ |
| $B_1$ | 1124.07 | 1124.37 | $\nu_{11}$ |
| $B_2$ | 1146.00 | 1146.19 | $\nu_{14}$ |
| $A_2$ | 1148.22 | 1148.40 | $\nu_7$ |
| $A_1$ | 1270.95 | 1270.94 | $\nu_3$ |
| $B_1$ | 1467.59 | 1467.72 | $\nu_{10}$ |
| $A_1$ | 1495.49 | 1495.74 | $\nu_2$ |
| $A_1$ | 1588.03 | 1589.09 | $2\nu_{15}$ |
| $A_2$ | 1611.50 | 1611.63 | $\nu_{15} + \nu_{12}$ |
| $A_1$ | 1641.39 | 1641.21 | $2\nu_{12}$ |
| $B_2$ | 1670.69 | 1670.78 | $\nu_{15} + \nu_5$ |
| $B_1$ | 1695.36 | 1695.13 | $\nu_5 + \nu_{12}$ |
| $A_1$ | 1755.07 | 1754.81 | $2\nu_5$ |
| $B_1$ | 1806.39 | 1806.81 | $\nu_{15} + \nu_8$ |
| $B_2$ | 1832.96 | 1832.89 | $\nu_{12} + \nu_8$ |
| $A_2$ | 1889.73 | 1889.81 | $\nu_5 + \nu_8$ |
| $A_2$ | 1908.54 | 1908.90 | $\nu_{15} + \nu_{11}$ |
| $B_2$ | 1910.58 | 1910.80 | $\nu_{15} + \nu_4$ |
| $B_1$ | 1928.71 | 1929.15 | $\nu_{15} + \nu_7$ |
| $A_1$ | 1938.65 | 1938.92 | $\nu_{15} + \nu_{14}$ |
| $B_1$ | 1940.37 | 1940.58 | $\nu_{12} + \nu_4$ |
| $A_1$ | 1944.67 | 1944.71 | $\nu_{12} + \nu_{11}$ |
| $A_2$ | 1962.19 | 1962.04 | $\nu_{12} + \nu_{14}$ |
| $B_2$ | 1970.84 | 1970.60 | $\nu_{12} + \nu_7$ |
| $A_1$ | 1998.09 | 1997.73 | $\nu_5 + \nu_4$ |
| $B_1$ | 1999.74 | 1999.39 | $\nu_5 + \nu_{11}$ |
| $B_2$ | 2021.35 | 2021.12 | $\nu_5 + \nu_{14}$ |
| $A_2$ | 2024.24 | 2024.00 | $\nu_5 + \nu_7$ |
| $A_1$ | 2032.16 | 2032.78 | $2\nu_8$ |
| $B_2$ | 2060.62 | 2060.74 | $\nu_{15} + \nu_3$ |
| $B_1$ | 2086.60 | 2086.38 | $\nu_{12} + \nu_3$ |
| $A_2$ | 2128.92 | 2128.77 | $\nu_8 + \nu_4$ |
| $B_2$ | 2135.29 | 2135.21 | $\nu_8 + \nu_{11}$ |
| $A_1$ | 2140.80 | 2140.60 | $\nu_5 + \nu_3$ |
| $B_1$ | 2152.76 | 2152.89 | $\nu_8 + \nu_{14}$ |
| $A_1$ | 2165.51 | 2165.40 | $\nu_8 + \nu_7$ |
| $A_1$ | 2236.23 | 2236.66 | $2\nu_4$ |
| $B_1$ | 2242.75 | 2243.99 | $\nu_4 + \nu_{11}$ |
| $A_2$ | 2246.58 | 2247.45 | $\nu_{15} + \nu_{10}$ |
| $A_1$ | 2249.90 | 2250.81 | $2\nu_{11}$ |
| $B_2$ | 2264.70 | 2266.13 | $\nu_7 + \nu_{11}$ |
| $A_2$ | *2267.87* | *2268.95* | $\nu_{14} + \nu_{11}$ |
| $B_2$ | *2268.07* | *2268.67* | $\nu_{14} + \nu_4$ |
| $A_2$ | 2275.16 | 2275.77 | $\nu_7 + \nu_4$ |
| $B_2$ | 2282.99 | 2284.58 | $\nu_{15} + \nu_2$ |
| $A_1$ | 2288.29 | 2288.50 | $\nu_{12} + \nu_{10}$ |
| $A_2$ | 2289.88 | 2290.67 | $\nu_3 + \nu_8$ |
| $A_1$ | 2290.79 | 2291.41 | $2\nu_{14}$ |
| $B_1$ | 2293.56 | 2294.02 | $\nu_7 + \nu_{14}$ |
| $A_1$ | 2296.10 | 2296.40 | $2\nu_7$ |
| $B_1$ | 2310.81 | 2311.26 | $\nu_{12} + \nu_2$ |
| $B_1$ | 2345.42 | 2345.49 | $\nu_5 + \nu_{10}$ |
| $A_1$ | 2370.35 | 2370.74 | $\nu_5 + \nu_2$ |
| $B_2$ | 2381.33 | **2388.00** | $3\nu_{15}$ |
| $A_1$ | 2389.76 | 2389.51 | $\nu_3 + \nu_4$ |
| $B_1$ | 2391.37 | 2391.01 | $\nu_3 + \nu_{11}$ |
| $B_1$ | 2402.50 | 2405.27 | $2\nu_{15} + \nu_{12}$ |
| $B_2$ | 2415.20 | 2415.12 | $\nu_3 + \nu_{14}$ |
| $A_2$ | 2415.99 | 2415.73 | $\nu_3 + \nu_7$ |
| $B_2$ | 2428.33 | 2429.22 | $\nu_{15} + 2\nu_{12}$ |
| $B_1$ | 2458.05 | 2458.83 | $3\nu_{12}$ |
| $A_1$ | 2465.15 | 2468.36 | $2\nu_{15} + \nu_5$ |

*continued on next page*

*continued on next page*

| irreps. | VMFCI(11956.6) | Ref. 1 | Assignment[1] |
|---|---|---|---|
| $B_2$ | 2481.23 | 2482.05 | $\nu_{10}+\nu_8$ |
| $A_2$ | 2484.11 | 2484.74 | $\nu_{15}+\nu_5+\nu_{12}$ |
| $A_2$ | 2506.69 | 2507.98 | $\nu_2+\nu_8$ |
| $A_1$ | 2510.12 | 2513.46 | $\nu_5+2\nu_{12}$ |
| $A_1$ | 2537.36 | 2537.41 | $2\nu_3$ |
| $B_2$ | 2546.70 | 2547.55 | $\nu_{15}+2\nu_5$ |
| $B_1$ | 2567.16 | 2567.33 | $2\nu_5+\nu_{12}$ |
| $B_1$ | 2583.86 | 2584.32 | $\nu_{10}+\nu_4$ |
| $A_1$ | 2587.72 | 2588.24 | $\nu_{10}+\nu_{11}$ |
| $A_2$ | 2595.27 | 2597.09 | $2\nu_{15}+\nu_8$ |
| $A_2$ | 2599.54 | 2600.34 | $\nu_{10}+\nu_{14}$ |
| $B_2$ | 2601.60 | 2602.28 | $\nu_{10}+\nu_7$ |
| $A_1$ | 2612.35 | 2613.87 | $\nu_2+\nu_4$ |
| $B_1$ | 2616.37 | 2617.02 | $\nu_2+\nu_{11}$ |
| $A_1$ | 2616.89 | 2618.09 | $\nu_{15}+\nu_{12}+\nu_8$ |
| $A_1$ | 2629.75 | 2630.88 | $3\nu_5$ |
| $A_2$ | 2640.84 | 2641.75 | $\nu_2+\nu_7$ |
| $B_2$ | 2641.13 | 2641.91 | $\nu_2+\nu_{14}$ |
| $A_2$ | 2646.04 | 2646.24 | $2\nu_{12}+\nu_8$ |
| $B_1$ | 2676.07 | 2677.43 | $\nu_{15}+\nu_5+\nu_8$ |
| $B_1$ | 2693.79 | 2696.02 | $2\nu_{15}+\nu_{11}$ |
| $A_1$ | *2699.42* | *2701.69* | $2\nu_{15}+\nu_4$ |
| $B_2$ | *2700.39* | *2701.38* | $\nu_5+\nu_{12}+\nu_8$ |
| $A_2$ | 2711.51 | 2713.94 | $2\nu_{15}+\nu_7$ |
| $B_2$ | 2721.54 | 2723.68 | $\nu_{15}+\nu_{12}+\nu_{11}$ |
| $A_2$ | 2728.32 | 2730.67 | $\nu_{15}+\nu_{12}+\nu_4$ |
| $B_2$ | 2734.81 | 2736.72 | $2\nu_{15}+\nu_{14}$ |
| $B_1$ | 2736.84 | 2737.37 | $\nu_{10}+\nu_3$ |
| $A_1$ | 2743.92 | 2744.96 | $\nu_{15}+\nu_{12}+\nu_7$ |
| $B_1$ | 2751.45 | 2752.71 | $\nu_{15}+\nu_{12}+\nu_{14}$ |
| $A_1$ | 2757.10 | 2758.29 | $2\nu_{12}+\nu_4$ |
| $A_2$ | 2760.48 | 2761.35 | $2\nu_5+\nu_8$ |
| $B_1$ | 2760.82 | 2761.37 | $2\nu_{12}+\nu_{11}$ |
| $A_1$ | 2762.81 | 2763.88 | $\nu_2+\nu_3$ |
| $B_2$ | 2775.18 | 2775.59 | $2\nu_{12}+\nu_{14}$ |
| $A_2$ | 2784.06 | 2787.72 | $\nu_{15}+\nu_5+\nu_{11}$ |
| $B_2$ | 2785.74 | 2788.41 | $\nu_{15}+\nu_5+\nu_4$ |
| $A_2$ | 2789.89 | 2790.40 | $2\nu_{12}+\nu_7$ |
| $B_1$ | 2803.09 | **2809.98** | $\nu_{15}+\nu_5+\nu_7$ |
| $A_1$ | 2811.45 | 2813.50 | $\nu_5+\nu_{12}+\nu_{11}$ |
| $A_1$ | 2812.63 | 2817.12 | $\nu_{15}+\nu_5+\nu_{14}$ |
| $B_2$ | 2815.48 | 2817.46 | $\nu_{15}+2\nu_8$ |
| $B_1$ | 2816.02 | 2817.70 | $\nu_5+\nu_{12}+\nu_4$ |
| $A_2$ | 2832.39 | 2834.71 | $\nu_5+\nu_{12}+\nu_{14}$ |
| $B_1$ | *2840.51* | *2842.50* | $\nu_{12}+2\nu_8$ |
| $B_2$ | *2841.30* | *2842.15* | $\nu_5+\nu_{12}+\nu_7$ |
| $A_1$ | 2851.94 | 2853.47 | $2\nu_{15}+\nu_3$ |
| $A_1$ | 2872.12 | 2873.05 | $2\nu_5+\nu_4$ |
| $A_2$ | *2872.23* | *2874.54* | $\nu_{15}+\nu_{12}+\nu_3$ |
| $B_1$ | *2872.96* | *2873.88* | $2\nu_5+\nu_{11}$ |
| $B_2$ | 2894.46 | 2895.89 | $2\nu_5+\nu_{14}$ |
| $A_2$ | 2897.94 | 2898.62 | $2\nu_5+\nu_7$ |
| $A_1$ | 2898.22 | 2901.60 | $\nu_5+2\nu_8$ |
| $A_1$ | 2900.68 | 2902.18 | $2\nu_{12}+\nu_3$ |
| $B_1$ | 2907.72 | 2911.04 | $\nu_9$ |
| $A_1$ | 2913.03 | 2917.53 | $\nu_{15}+\nu_8+\nu_{11}$ [a] |
| $B_1$ | 2915.00 | 2917.90 | $\nu_{15}+\nu_8+\nu_4$ |

*continued on next page*

| irreps. | VMFCI(11956.6) | Ref. 1 | Assignment[1] |
|---|---|---|---|
| $A_1$ | 2918.79 | 2923.02 | $\nu_1$ |
| $B_2$ | 2929.63 | 2932.84 | $\nu_{15}+\nu_5+\nu_3$ |
| $B_2$ | 2934.76 | 2937.33 | $\nu_{12}+\nu_8+\nu_4$ |
| $A_2$ | 2940.11 | 2942.52 | $\nu_{15}+\nu_8+\nu_{14}$ |
| $B_2$ | 2946.04 | 2949.06 | $\nu_{15}+\nu_8+\nu_7$ |
| $A_2$ | 2949.03 | 2951.56 | $\nu_{12}+\nu_8+\nu_{11}$ |
| $B_1$ | 2952.56 | 2954.44 | $\nu_5+\nu_{12}+\nu_3$ |
| $A_1$ | 2953.40 | 2958.32 | $2\nu_{10}$ |
| $A_1$ | 2965.35 | 2967.45 | $\nu_{12}+\nu_8+\nu_{14}$ |
| $B_1$ | 2980.82 | 2981.94 | $\nu_{12}+\nu_8+\nu_7$ |
| $B_1$ | 2990.72 | 2995.63 | $\nu_2+\nu_{10}$ |
| $A_1$ | *2995.54* | ***3002.34*** | $2\nu_2$ |
| $A_2$ | *2999.17* | *3000.44* | $\nu_5+\nu_8+\nu_4$ |
| $B_2$ | 3003.31 | 3006.30 | $\nu_5+\nu_8+\nu_{11}$ |
| $A_1$ | 3009.07 | 3009.47 | $2\nu_5+\nu_3$ |
| $B_2$ | 3013.56 | **3020.05** | $\nu_{15}+2\nu_{11}$ [c1] |
| $A_2$ | *3021.24* | *3025.44* | $\nu_{15}+\nu_4+\nu_{11}$ |
| $B_1$ | *3023.14* | *3024.79* | $\nu_5+\nu_8+\nu_{14}$ |
| $A_2$ | 3026.36 | 3027.95 | $\nu_6$ |
| $B_2$ | 3030.94 | 3033.86 | $\nu_{15}+2\nu_4$ [c1] |
| $B_1$ | *3034.01* | *3038.36* | $2\nu_{15}+\nu_{10}$ |
| $A_1$ | *3034.03* | *3035.70* | $\nu_5+\nu_8+\nu_7$ |
| $B_2$ | 3038.39 | 3040.21 | $\nu_{13}$ |
| $A_2$ | *3041.93* | ***3048.87*** | $3\nu_8$ |
| $A_1$ | 3042.71 | **3048.70** | $\nu_{15}+\nu_7+\nu_{11}$ |
| $B_1$ | *3043.77* | *3048.42* | $\nu_{12}+2\nu_{11}$ [b] |
| $B_1$ | 3050.73 | **3057.21** | $\nu_{15}+\nu_{14}+\nu_{11}$ |
| $A_1$ | 3053.21 | **3060.39** | $\nu_{12}+\nu_4+\nu_{11}$ |
| $A_1$ | 3056.21 | **3061.69** | $\nu_{15}+\nu_{14}+\nu_4$ |
| $B_1$ | 3060.53 | **3066.08** | $\nu_{15}+\nu_7+\nu_4$ |
| $B_2$ | 3063.15 | 3066.94 | $\nu_{15}+\nu_{12}+\nu_{10}$ |
| $A_1$ | *3063.78* | ***3071.18*** | $2\nu_{15}+\nu_2$ |
| $B_1$ | *3065.83* | *3069.95* | $\nu_{12}+2\nu_4$ [b] |
| $A_2$ | *3069.09* | ***3074.73*** | $\nu_{12}+\nu_{14}+\nu_4$ [d] |
| $B_2$ | *3069.29* | *3072.99* | $\nu_{15}+2\nu_{14}$ [c2] |
| $B_1$ | 3074.08 | **3079.51** | $\nu_{15}+\nu_3+\nu_8$ |
| $A_2$ | *3079.24* | ***3085.65*** | $\nu_{15}+\nu_{12}+\nu_2$ |
| $B_2$ | *3080.70* | *3084.54* | $\nu_{12}+\nu_{14}+\nu_{11}$ |
| $A_2$ | 3083.97 | 3088.11 | $\nu_{15}+\nu_7+\nu_{14}$ |
| $B_2$ | 3085.07 | 3088.58 | $\nu_{15}+2\nu_7$ [c2] |
| $B_2$ | 3092.78 | **3098.61** | $\nu_{12}+\nu_7+\nu_4$ |
| $A_2$ | 3099.06 | 3102.95 | $\nu_{12}+\nu_7+\nu_{11}$ |
| $B_2$ | 3100.52 | 3103.16 | $\nu_{12}+\nu_3+\nu_8$ |
| $B_1$ | 3100.73 | 3104.30 | $\nu_{12}+2\nu_{14}$ |
| $B_1$ | 3106.74 | 3109.15 | $2\nu_{12}+\nu_{10}$ |
| $A_1$ | *3109.44* | ***3115.58*** | $\nu_{12}+\nu_7+\nu_{14}$ [e] |
| $A_1$ | *3109.53* | ***3125.67*** | $\nu_5+2\nu_4$ [e] |
| $B_1$ | 3114.87 | 3119.83 | $\nu_5+\nu_4+\nu_{11}$ |
| $B_1$ | 3118.20 | 3121.56 | $\nu_{12}+2\nu_7$ |
| $A_1$ | *3121.77* | ***3112.80*** | $\nu_5+2\nu_{11}$ [e] |
| $A_2$ | 3122.74 | 3125.96 | $\nu_{15}+\nu_5+\nu_{10}$ |
| $A_1$ | 3125.17 | 3127.61 | $2\nu_{12}+\nu_2$ |
| $A_1$ | 3131.40 | 3134.62 | $2\nu_8+\nu_4$ |
| $A_2$ | *3137.83* | ***3143.98*** | $\nu_5+\nu_{14}+\nu_{11}$ |
| $B_2$ | *3138.43* | *3141.97* | $\nu_5+\nu_7+\nu_{11}$ |
| $B_2$ | *3140.71* | *3142.77* | $\nu_5+\nu_{14}+\nu_4$ |
| $B_1$ | 3141.72 | 3146.30 | $2\nu_8+\nu_{11}$ |

*continued on next page*

| irreps. | VMFCI(11956.6) | Ref. 1 | Assignment[1] |
|---|---|---|---|
| $A_2$ | 3148.76 | **3154.15** | $\nu_5+\nu_7+\nu_4$ |
| $A_2$ | 3155.47 | **3160.67** | $\nu_5+\nu_3+\nu_8$ |
| $B_2$ | 3156.27 | **3162.47** | $\nu_{15}+\nu_5+\nu_2$ |
| $B_2$ | 3156.67 | **3163.50** | $2\nu_8+\nu_{14}$ |
| $A_1$ | 3160.98 | 3163.70 | $\nu_5+\nu_{12}+\nu_{10}$ |
| $A_1$ | 3162.51 | 3164.77 | $\nu_5+2\nu_{14}$ |
| $B_1$ | 3165.89 | 3169.44 | $\nu_5+\nu_7+\nu_{14}$ |
| $A_1$ | 3168.96 | 3171.54 | $\nu_5+2\nu_7$ |
| $A_1$ | 3170.54 | ??? | $4\nu_{15}$ |
| $A_2$ | 3171.59 | 3175.51 | $\nu_{15}+\nu_3+\nu_{11}$ |
| $B_2$ | 3175.16 | 3179.51 | $\nu_{15}+\nu_3+\nu_4$ |
| $A_2$ | 3178.65 | 3182.09 | $2\nu_8+\nu_7$ |
| $B_1$ | 3181.45 | **3189.11** | $\nu_5+\nu_{12}+\nu_2$ |
| $A_2$ | 3190.24 | ??? | $3\nu_{15}+\nu_{12}$ |
| $B_1$ | 3192.71 | **3198.95** | $\nu_{15}+\nu_3+\nu_7$ |
| $A_1$ | 3201.63 | 3205.73 | $\nu_{12}+\nu_3+\nu_{11}$ |
| $B_1$ | 3201.86 | 3206.84 | $\nu_{12}+\nu_3+\nu_4$ |
| $A_1$ | 3206.74 | 3209.19 | $\nu_{15}+\nu_3+\nu_{14}$ |
| $A_1$ | 3216.11 | ??? | $2\nu_5+2\nu_{12}$ |
| $B_1$ | 3221.25 | 3225.03 | $2\nu_5+\nu_{10}$ |
| $A_2$ | 3224.44 | 3227.09 | $\nu_{12}+\nu_3+\nu_{14}$ |
| $B_2$ | 3231.59 | 3235.46 | $\nu_{12}+\nu_3+\nu_7$ |

Table I. Inverted or permuted wave numbers are italicized, the HI-RRBPM numbers which deviate by more than 5 $cm^{-1}$ are in bold. Some wave numbers are missing in the HI-RRBPM list and are marked by the symbol ???. This is probably because they would appear higher in the spectrum. They are overtones or combinations bands of low frequency modes which does not seem to be well described in the HI-RRBPM calculation arguably due to too low basis truncation criteria. As a matter of fact, most of the bold number correspond to bands involving $\nu_5$, $\nu_{12}$ or $\nu_{15}$. Some footnotes in this tables are related to those in Tab. 2 of Ref. 1.

[a] main weight on $\nu_1$ in VMFCI calculation, as for the eigenstate corresponding to 2918.79 $cm^{-1}$.
[b] both assignments to $\nu_{12}+2\nu_{11}$ in the new calculation.
[c1,c2] inversion confirmed in the new calculation.
[d] still assigned to $\nu_{15}+\nu_7+\nu_{14}$ in the new calculation.
[e] permutation of 3 levels in the new calculation instead of just 2.

### C. Comparison of the new VMFCI reference calculation with a previous VMFCI calculation using a different contraction-truncation scheme

Here, we display the 200 lowest eigenvalues of the new VMFCI calculation used as a reference for the AnharmoniCaOs calculations in the main text. It is compared to a previous VMFCI calculation, referred to as VMFCI(11300), which uses force field 2 but was compared to force field 3 HI-RRBPM calculations in Ref 1.

The contraction-truncation schemes of the two calculations are different. The contraction-truncation scheme of the new VMFCI(11956.6) calculation is the same as that of the previous section except that the 2-contraction step VMFCI($\{\{\nu_1,\nu_6,\nu_9,\nu_{13}\}_{17523},\{\nu_2,\nu_{10}\}_{12272},\{\nu_8,\nu_{15}\}_{12077}\}$, 17914; $\{\{\nu_3,\nu_5,\nu_{12}\}_{11459},\{\nu_4,\nu_{11}\}_{11156},\{\nu_7,\nu_{14}\}_{9633}\}$, 15280 ), is iterated once, leading to a common ZPE for the two contractions of $12492.353 \pm 0.001$ $cm^{-1}$. This ZPE is to be compared with that of the 6-contraction VSCFCI step of $12502.883 \pm 0.001$ $cm^{-1}$and with the converged VSCF ZPE of 12540.280269 $cm^{-1}$.
The size of the final VCI is 429499 splitted into 4 $C_{2V}$-symmetry blocks of dimensions 107852 for A1, 107096 for A2, 107415 for B1, 107136 for B2.

The contraction-truncation scheme of the old VMFCI(11300) calculation is essentially the same as that of Ref. 2, with a larger final threshold: 11300 $cm^{-1}$ instead of 10721 $cm^{-1}$. It can be abbreviated as:
VSCF/VSCFCI($\{\nu_1,\nu_6,\nu_9,\nu_{13}\}$, 34072; $\{\nu_3,\nu_5,\nu_{12}\}$, 17000)/VSCFCI($\{\{\nu_1,\nu_6,\nu_9,\nu_{13}\},\nu_{10},\nu_{15}\}$, 19464)/VCI(11300)
The size of the final VCI is larger than for the new one with 456201 basis functions splitted into 4 $C_{2V}$-symmetry blocks of dimensions 114852 for A1, 113489 for A2, 114278 for B1, 113582 for B2. However, the results are clearly less accurate (see Table S2 below).

TABLE II: Lowest 200 vibrational energy levels (in $cm^{-1}$) of ethylene oxide for force field 2

| irreps. | VMFCI(11956.6) | VMFCI(11300)[1] |
|---|---|---|
| $A_1$ | 12463.57 | 12463.65 |
| $B_2$ | 793.03 | 793.37 |
| $B_1$ | 822.48 | 822.75 |
| $A_1$ | 878.76 | 879.04 |
| $A_2$ | 1017.97 | 1018.96 |
| $A_1$ | 1122.14 | 1122.96 |
| $B_1$ | 1124.37 | 1125.18 |
| $B_2$ | 1146.45 | 1147.09 |
| $A_2$ | 1148.42 | 1149.02 |
| $A_1$ | 1271.11 | 1271.50 |
| $B_1$ | 1467.98 | 1468.34 |
| $A_1$ | 1496.00 | 1496.65 |
| $A_1$ | 1588.62 | 1589.38 |
| $A_2$ | 1612.27 | 1612.92 |
| $A_1$ | 1642.48 | 1642.86 |
| $B_2$ | 1671.38 | 1671.94 |
| $B_1$ | 1696.43 | 1696.71 |
| $A_1$ | 1755.98 | 1756.21 |
| $B_1$ | 1807.45 | 1808.96 |
| $B_2$ | 1834.31 | 1835.47 |
| $A_2$ | 1890.96 | 1891.96 |

*continued on next page*

| irreps. | VMFCI(11956.6) | VMFCI(11300)[1] |
|---|---|---|
| $A_2$ | 1909.35 | 1910.19 |
| $B_2$ | 1911.54 | 1912.38 |
| $B_1$ | 1929.48 | 1930.21 |
| $A_1$ | 1939.41 | 1940.01 |
| $B_1$ | 1941.36 | 1941.82 |
| $A_1$ | 1945.44 | 1945.80 |
| $A_2$ | 1963.29 | 1963.62 |
| $B_2$ | 1971.50 | 1971.83 |
| $A_1$ | 1999.08 | 1999.34 |
| $B_1$ | 2000.51 | 2000.76 |
| $B_2$ | 2022.30 | 2022.57 |
| $A_2$ | 2024.90 | 2025.19 |
| $A_1$ | 2033.60 | 2036.08 |
| $B_2$ | 2061.03 | 2061.51 |
| $B_1$ | 2087.26 | 2087.49 |
| $A_2$ | 2130.39 | 2132.05 |
| $B_2$ | 2136.49 | 2138.11 |
| $A_1$ | 2141.59 | 2141.80 |
| $B_1$ | 2154.23 | 2155.72 |
| $A_1$ | 2166.39 | 2167.73 |
| $A_1$ | 2237.29 | 2237.65 |
| $B_1$ | 2243.54 | 2243.80 |
| $A_2$ | 2247.41 | 2247.97 |
| $A_1$ | 2250.51 | 2250.86 |
| $B_2$ | 2265.43 | 2266.28 |
| $A_2$ | 2268.70 | 2269.27 |
| $B_2$ | 2269.00 | 2269.43 |
| $A_2$ | 2275.80 | 2276.17 |
| $B_2$ | 2283.65 | 2284.40 |
| $A_1$ | 2289.19 | 2289.57 |
| $A_2$ | 2290.60 | 2291.52 |
| $A_1$ | 2291.68 | 2292.21 |
| $B_1$ | 2294.23 | 2294.73 |
| $A_1$ | 2296.53 | 2297.09 |
| $B_1$ | 2311.89 | 2312.71 |
| $B_1$ | 2346.25 | 2346.58 |
| $A_1$ | 2371.38 | 2372.12 |
| $B_2$ | 2382.39 | 2382.86 |
| $A_1$ | 2390.42 | 2390.76 |
| $B_1$ | 2391.82 | 2392.13 |
| $B_1$ | 2403.66 | 2404.62 |
| $B_2$ | 2415.82 | 2416.22 |
| $A_2$ | 2416.33 | 2416.72 |
| $B_2$ | 2429.68 | 2430.50 |
| $B_1$ | 2459.82 | 2460.42 |
| $A_1$ | 2466.23 | 2467.01 |
| $B_2$ | 2482.36 | 2483.52 |
| $A_2$ | 2485.46 | 2486.14 |
| $A_2$ | 2508.00 | 2510.34 |
| $A_1$ | 2511.90 | 2512.47 |
| $A_1$ | 2537.63 | 2538.02 |
| $B_2$ | 2547.89 | 2548.58 |
| $B_1$ | 2568.81 | 2569.28 |
| $B_1$ | 2584.82 | 2585.75 |
| $A_1$ | 2588.50 | 2589.46 |
| $A_2$ | 2596.91 | 2599.54 |
| $A_2$ | 2600.64 | 2601.69 |

*continued on next page*

| irreps. | VMFCI(11956.6) | VMFCI(11300)[1] |
|---|---|---|
| $B_2$ | 2602.50 | 2603.53 |
| $A_1$ | 2613.54 | 2615.39 |
| $B_1$ | 2617.19 | 2618.85 |
| $A_1$ | 2618.61 | 2621.28 |
| $A_1$ | 2631.18 | 2631.55 |
| $A_2$ | 2641.56 | 2643.15 |
| $B_2$ | 2642.02 | 2643.48 |
| $A_2$ | 2648.15 | 2650.27 |
| $B_1$ | 2677.78 | 2680.29 |
| $B_1$ | 2695.22 | 2697.64 |
| $A_1$ | 2700.93 | 2703.48 |
| $B_2$ | 2702.44 | 2704.29 |
| $A_2$ | 2712.80 | 2715.21 |
| $B_2$ | 2722.99 | 2725.03 |
| $A_2$ | 2729.73 | 2731.66 |
| $B_2$ | 2735.91 | 2737.56 |
| $B_1$ | 2737.38 | 2737.96 |
| $A_1$ | 2745.45 | 2747.23 |
| $B_1$ | 2752.86 | 2754.35 |
| $A_1$ | 2758.55 | 2760.02 |
| $B_1$ | 2762.24 | 2763.28 |
| $A_2$ | 2762.32 | 2763.83 |
| $A_1$ | 2763.49 | 2764.81 |
| $B_2$ | 2777.03 | 2778.08 |
| $A_2$ | 2785.37 | 2786.85 |
| $B_2$ | 2787.21 | 2788.85 |
| $A_2$ | 2791.15 | 2792.07 |
| $B_1$ | 2804.45 | 2805.89 |
| $A_1$ | 2812.84 | 2813.86 |
| $B_1$ | 2814.12 | 2815.20 |
| $A_1$ | 2817.31 | 2818.25 |
| $B_2$ | 2817.53 | **2822.93** |
| $A_2$ | 2834.11 | 2834.86 |
| $B_2$ | 2842.57 | 2843.35 |
| $B_1$ | 2842.87 | 2847.79 |
| $A_1$ | 2852.76 | 2854.33 |
| $A_2$ | *2873.20* | *2874.44* |
| $A_1$ | *2873.63* | *2874.30* |
| $B_1$ | 2874.26 | 2874.81 |
| $B_2$ | 2895.96 | 2896.62 |
| $A_2$ | 2899.13 | 2899.84 |
| $A_1$ | 2900.38 | **2905.43** |
| $A_1$ | 2901.94 | 2902.67 |
| $B_1$ | 2909.55 | 2910.86 |
| $A_1$ | 2914.73 | 2916.69 |
| $B_1$ | 2916.95 | **2922.14** |
| $A_1$ | 2920.29 | 2924.52 |
| $B_2$ | 2930.71 | 2931.82 |
| $B_2$ | 2936.85 | 2941.73 |
| $A_2$ | 2942.08 | 2946.78 |
| $B_2$ | 2947.75 | 2951.93 |
| $A_2$ | 2950.91 | 2954.90 |
| $B_1$ | 2953.94 | 2954.55 |
| $A_1$ | 2955.01 | 2956.38 |
| $A_1$ | 2967.42 | 2971.25 |
| $B_1$ | 2982.39 | 2985.81 |
| $B_1$ | 2992.22 | 2993.97 |

*continued on next page*

| irreps. | VMFCI(11956.6) | VMFCI(11300)[1] |
|---|---|---|
| $A_1$ | 2997.03 | 3000.08 |
| $A_2$ | 3001.27 | 3005.26 |
| $B_2$ | 3005.13 | 3009.46 |
| $A_1$ | 3010.51 | 3011.16 |
| $B_2$ | 3015.27 | **3020.67** |
| $A_2$ | 3022.83 | 3027.65 |
| $B_1$ | 3025.19 | 3028.81 |
| $A_2$ | 3028.63 | 3029.75 |
| $B_2$ | 3032.42 | 3035.82 |
| $B_1$ | 3035.32 | 3038.05 |
| $A_1$ | 3035.53 | 3039.04 |
| $B_2$ | 3040.60 | 3041.99 |
| $A_1$ | 3043.97 | 3047.88 |
| $A_2$ | *3044.37* | ***3055.15*** |
| $B_1$ | *3045.56* | *3049.21* |
| $B_1$ | 3052.13 | 3055.92 |
| $A_1$ | 3054.74 | 3057.68 |
| $A_1$ | 3057.67 | 3061.06 |
| $B_1$ | 3061.83 | 3064.98 |
| $B_2$ | 3064.57 | 3066.76 |
| $A_1$ | 3065.11 | 3068.03 |
| $B_1$ | 3066.99 | 3069.49 |
| $B_2$ | 3070.40 | 3073.86 |
| $A_2$ | 3070.63 | 3073.86 |
| $B_1$ | 3075.31 | 3078.94 |
| $A_2$ | 3080.74 | 3084.02 |
| $B_2$ | 3082.16 | 3084.92 |
| $A_2$ | 3085.30 | 3087.97 |
| $B_2$ | 3086.36 | 3089.06 |
| $B_2$ | 3093.99 | 3096.23 |
| $A_2$ | 3100.17 | 3102.56 |
| $B_2$ | 3101.89 | 3104.44 |
| $B_1$ | 3102.46 | 3105.97 |
| $B_1$ | 3108.24 | 3109.55 |
| $A_1$ | 3110.78 | 3112.92[b] |
| $A_1$ | 3111.10 | **3116.35** |
| $B_1$ | 3116.21 | 3118.38 |
| $B_1$ | 3119.06 | 3122.34 |
| $A_1$ | 3122.94 | 3127.59 |
| $A_2$ | 3124.07 | 3126.44 |
| $A_1$ | 3126.88 | 3129.22 |
| $A_1$ | *3134.00* | ***3146.79*** |
| $A_2$ | *3139.32* | *3143.09* |
| $B_2$ | *3139.67* | *3143.48* |
| $B_2$ | *3142.20* | *3146.04* |
| $B_1$ | *3143.98* | ***3156.68*** |
| $A_2$ | *3149.94* | *3153.20* |
| $A_2$ | 3156.84 | 3159.94 |
| $B_2$ | 3157.70 | 3160.91 |
| $B_2$ | *3159.06* | ***3170.99*** |
| $A_1$ | *3162.45* | *3163.64* |
| $A_1$ | *3164.00* | *3168.19* |
| $B_1$ | *3167.12* | *3170.35* |
| $A_1$ | 3169.90 | 3173.84 |
| $A_1$ | 3172.17 | 3174.28 |
| $A_2$ | 3172.61 | 3175.82 |
| $B_2$ | 3176.29 | 3179.58 |
| $A_2$ | *3180.39* | ***3190.21*** |
| $B_1$ | *3183.15* | *3186.27* |
| $A_2$ | 3191.97 | 3195.37 |
| $B_1$ | 3193.72 | 3197.44 |
| $A_1$ | 3202.65 | 3206.44 |
| $B_1$ | 3202.99 | 3206.78 |
| $A_1$ | 3207.67 | 3210.84 |
| $A_1$ | *3217.88* | ??? [a] |
| $B_1$ | 3222.57 | 3223.58 |
| $A_2$ | 3225.77 | 3229.36 |
| $B_2$ | 3232.42 | 3235.64 |

*continued on next page*

Table II. Inverted or permuted wave numbers are italicized, the VMFCI(11300) numbers which deviate by more than 5 $cm^{-1}$ are in bold. Some wave numbers are missing in the VMFCI(11300) list and are marked by the symbol ???. This is because they appear higher in the spectrum. As a matter of fact, the quality of the VMFCI(11300) calculation deteriorate beyond 3110 $cm^{-1}$ where many bold and italicized numbers appear. Some footnotes in this tables are related to those in Tab.2 of Ref. 1.

[a] assigned to $2\nu_5 + 2\nu_{12}$ in the new calculation, missing in the old one.
[b] this wave number is assigned to $\nu_{12} + \nu_8 + \nu_{15}$ in the new calculation and to $\nu_{12} + \nu_7 + \nu_{14}$ in the old one.

## II. HARMONIC VIBRATIONAL ANALYSES

The cubic and quartic force field constants, as well as the first and second electric dipole moment derivatives that our AnharmoniCaOs code uses were obtained via DFT calculations with the B97-1 exchange-correlation functional with the TZ2P and 6-31G* Gaussian basis sets, as described in the text. Since we used numerical differentiation along normal coordinates, we give here the results of the harmonic vibrational analyses for both Pyrene (Table III) and Coronene (Table IV).

TABLE III: List of harmonic vibrational normal modes of Pyrene. For each mode numbered according to spectroscopic conventions, we list the irreducible representation label ("sym." column), the wave number in $cm^{-1}$, and the intensity of the corresponding fundamental IR transition in $km \cdot mol^{-1}$.

| | | B97-1/6-31g* | | B97-1/TZ2P | |
|---|---|---|---|---|---|
| mode | sym. | freq. | int. | freq. | int. |
| $\nu_1$ | $A_g$ | 3202.4 | 0.0 | 3182.2 | 0.0 |
| $\nu_2$ | $A_g$ | 3192.4 | 0.0 | 3172.8 | 0.0 |
| $\nu_3$ | $A_g$ | 3175.9 | 0.0 | 3157.5 | 0.0 |
| $\nu_4$ | $A_g$ | 1678.5 | 0.0 | 1661.0 | 0.0 |
| $\nu_5$ | $A_g$ | 1604.9 | 0.0 | 1587.8 | 0.0 |
| $\nu_6$ | $A_g$ | 1435.6 | 0.0 | 1420.8 | 0.0 |
| $\nu_7$ | $A_g$ | 1356.2 | 0.0 | 1347.3 | 0.0 |
| $\nu_8$ | $A_g$ | 1270.5 | 0.0 | 1256.9 | 0.0 |
| $\nu_9$ | $A_g$ | 1172.1 | 0.0 | 1164.9 | 0.0 |
| $\nu_{10}$ | $A_g$ | 1094.5 | 0.0 | 1085.6 | 0.0 |
| $\nu_{11}$ | $A_g$ | 809.8 | 0.0 | 811.3 | 0.0 |
| $\nu_{12}$ | $A_g$ | 594.6 | 0.0 | 593.2 | 0.0 |
| $\nu_{13}$ | $A_g$ | 409.6 | 0.0 | 409.6 | 0.0 |
| $\nu_{14}$ | $A_u$ | 969.0 | 0.0 | 985.1 | 0.0 |
| $\nu_{15}$ | $A_u$ | 896.2 | 0.0 | 908.2 | 0.0 |
| $\nu_{16}$ | $A_u$ | 685.5 | 0.0 | 689.7 | 0.0 |
| $\nu_{17}$ | $A_u$ | 400.9 | 0.0 | 399.9 | 0.0 |
| $\nu_{18}$ | $A_u$ | 153.1 | 0.0 | 149.9 | 0.0 |
| $\nu_{19}$ | $B_{1g}$ | 911.8 | 0.0 | 920.6 | 0.0 |
| $\nu_{20}$ | $B_{1g}$ | 816.5 | 0.0 | 815.4 | 0.0 |
| $\nu_{21}$ | $B_{1g}$ | 538.5 | 0.0 | 533.9 | 0.0 |
| $\nu_{22}$ | $B_{1g}$ | 250.3 | 0.0 | 246.9 | 0.0 |
| $\nu_{23}$ | $B_{1u}$ | 3202.0 | 71.116 | 3182.0 | 38.0 |
| $\nu_{24}$ | $B_{1u}$ | 3176.1 | 0.368 | 3157.8 | 0.0018 |
| $\nu_{25}$ | $B_{1u}$ | 3172.9 | 2.711 | 3154.4 | 1.2 |
| $\nu_{26}$ | $B_{1u}$ | 1643.2 | 12.622 | 1626.5 | 13.2 |
| $\nu_{27}$ | $B_{1u}$ | 1490.5 | 0.320 | 1478.9 | 1.0 |
| $\nu_{28}$ | $B_{1u}$ | 1466.4 | 11.194 | 1456.5 | 8.0 |
| $\nu_{29}$ | $B_{1u}$ | 1271.2 | 2.776 | 1264.3 | 2.3 |
| $\nu_{30}$ | $B_{1u}$ | 1117.8 | 5.675 | 1109.2 | 7.0 |
| $\nu_{31}$ | $B_{1u}$ | 1008.1 | 0.830 | 1011.5 | 1.8 |
| $\nu_{32}$ | $B_{1u}$ | 830.2 | 3.477 | 830.3 | 4.6 |
| $\nu_{33}$ | $B_{1u}$ | 700.6 | 0.151 | 700.8 | 0.029 |
| $\nu_{34}$ | $B_{1u}$ | 502.6 | 2.417 | 503.7 | 3.0 |
| $\nu_{35}$ | $B_{2g}$ | 980.0 | 0.0 | 990.7 | 0.0 |
| $\nu_{36}$ | $B_{2g}$ | 960.8 | 0.0 | 977.0 | 0.0 |
| $\nu_{37}$ | $B_{2g}$ | 837.2 | 0.0 | 859.2 | 0.0 |
| $\nu_{38}$ | $B_{2g}$ | 784.5 | 0.0 | 783.6 | 0.0 |
| $\nu_{39}$ | $B_{2g}$ | 583.0 | 0.0 | 586.5 | 0.0 |
| $\nu_{40}$ | $B_{2g}$ | 513.0 | 0.0 | 511.7 | 0.0 |
| $\nu_{41}$ | $B_{2g}$ | 264.2 | 0.0 | 259.7 | 0.0 |
| $\nu_{42}$ | $B_{2u}$ | 3192.1 | 69.930 | 3172.7 | 42.8 |
| $\nu_{43}$ | $B_{2u}$ | 3183.0 | 22.516 | 3165.0 | 12.7 |
| $\nu_{44}$ | $B_{2u}$ | 1653.6 | 4.393 | 1635.8 | 2.3 |
| $\nu_{45}$ | $B_{2u}$ | 1525.0 | 2.782 | 1508.5 | 3.2 |
| $\nu_{46}$ | $B_{2u}$ | 1466.2 | 2.046 | 1453.4 | 3.2 |
| $\nu_{47}$ | $B_{2u}$ | 1356.3 | 5.519 | 1338.3 | 4.9 |
| $\nu_{48}$ | $B_{2u}$ | 1236.1 | 0.026 | 1226.2 | 0.020 |
| $\nu_{49}$ | $B_{2u}$ | 1210.9 | 13.525 | 1202.2 | 14.0 |
| $\nu_{50}$ | $B_{2u}$ | 1174.7 | 0.418 | 1160.4 | 0.28 |

Continued on next page

TABLE III – continued from previous page

| | | B97-1/6-31g* | | B97-1/TZ2P | |
|---|---|---|---|---|---|
| mode | sym. | freq. | int. | freq. | int. |
| $\nu_{51}$ | $B_{2u}$ | 979.3 | 0.106 | 975.4 | 0.0025 |
| $\nu_{52}$ | $B_{2u}$ | 549.2 | 2.649 | 549.2 | 2.6 |
| $\nu_{53}$ | $B_{2u}$ | 355.8 | 1.327 | 356.5 | 1.7 |
| $\nu_{54}$ | $B_{3g}$ | 3183.4 | 0.0 | 3165.5 | 0.0 |
| $\nu_{55}$ | $B_{3g}$ | 3173.1 | 0.0 | 3154.6 | 0.0 |
| $\nu_{56}$ | $B_{3g}$ | 1632.6 | 0.0 | 1618.3 | 0.0 |
| $\nu_{57}$ | $B_{3g}$ | 1543.3 | 0.0 | 1528.9 | 0.0 |
| $\nu_{58}$ | $B_{3g}$ | 1443.4 | 0.0 | 1433.0 | 0.0 |
| $\nu_{59}$ | $B_{3g}$ | 1411.9 | 0.0 | 1393.9 | 0.0 |
| $\nu_{60}$ | $B_{3g}$ | 1264.6 | 0.0 | 1260.7 | 0.0 |
| $\nu_{61}$ | $B_{3g}$ | 1203.0 | 0.0 | 1194.9 | 0.0 |
| $\nu_{62}$ | $B_{3g}$ | 1125.4 | 0.0 | 1122.9 | 0.0 |
| $\nu_{63}$ | $B_{3g}$ | 744.4 | 0.0 | 745.2 | 0.0 |
| $\nu_{64}$ | $B_{3g}$ | 503.5 | 0.0 | 504.3 | 0.0 |
| $\nu_{65}$ | $B_{3g}$ | 459.2 | 0.0 | 459.7 | 0.0 |
| $\nu_{66}$ | $B_{3u}$ | 968.6 | 1.753 | 983.8 | 1.4 |
| $\nu_{67}$ | $B_{3u}$ | 859.3 | 109.082 | 860.0 | 111.9 |
| $\nu_{68}$ | $B_{3u}$ | 759.5 | 11.473 | 755.1 | 17.5 |
| $\nu_{69}$ | $B_{3u}$ | 722.5 | 25.863 | 725.6 | 44.8 |
| $\nu_{70}$ | $B_{3u}$ | 497.2 | 1.318 | 496.3 | 2.1 |
| $\nu_{71}$ | $B_{3u}$ | 216.2 | 6.968 | 210.2 | 10.6 |
| $\nu_{72}$ | $B_{3u}$ | 100.2 | 0.409 | 97.3 | 0.64 |

TABLE IV: List of harmonic vibrational normal modes of coronene. For each mode numbered according to spectroscopic conventions, we list the irreducible representation label ("sym." column), the wave number in $cm^{-1}$, and the intensity of the corresponding fundamental IR transition in $km \cdot mol^{-1}$

| | | B97-1/6-31g* | | B97-1/TZ2P | |
|---|---|---|---|---|---|
| mode | sym. | freq. | int. | freq. | int. |
| $\nu_1$ | $A_{1g}$ | 3194.3 | 0.0 | 3174.4 | 0.0 |
| $\nu_2$ | $A_{1g}$ | 1646.4 | 0.0 | 1629.3 | 0.0 |
| $\nu_3$ | $A_{1g}$ | 1385.1 | 0.0 | 1366.1 | 0.0 |
| $\nu_4$ | $A_{1g}$ | 1250.5 | 0.0 | 1240.7 | 0.0 |
| $\nu_5$ | $A_{1g}$ | 1048.4 | 0.0 | 1043.5 | 0.0 |
| $\nu_6$ | $A_{1g}$ | 483.9 | 0.0 | 483.0 | 0.0 |
| $\nu_7$ | $A_{1u}$ | 946.8 | 0.0 | 964.2 | 0.0 |
| $\nu_8$ | $A_{1u}$ | 526.4 | 0.0 | 530.4 | 0.0 |
| $\nu_9$ | $A_{2g}$ | 3172.8 | 0.0 | 3154.1 | 0.0 |
| $\nu_{10}$ | $A_{2g}$ | 1580.0 | 0.0 | 1565.2 | 0.0 |
| $\nu_{11}$ | $A_{2g}$ | 1257.7 | 0.0 | 1254.9 | 0.0 |
| $\nu_{12}$ | $A_{2g}$ | 931.2 | 0.0 | 941.2 | 0.0 |
| $\nu_{13}$ | $A_{2g}$ | 637.5 | 0.0 | 640.1 | 0.0 |
| $\nu_{14}$ | $A_{2u}$ | 873.5 | 158.034 | 873.2 | 167.908 |
| $\nu_{15}$ | $A_{2u}$ | 562.7 | 24.821 | 558.4 | 42.749 |
| $\nu_{16}$ | $A_{2u}$ | 128.0 | 4.784 | 123.4 | 6.911 |
| $\nu_{17}$ | $B_{1g}$ | 775.6 | 0.0 | 773.6 | 0.0 |
| $\nu_{18}$ | $B_{1g}$ | 166.1 | 0.0 | 162.9 | 0.0 |
| $\nu_{19}$ | $B_{1u}$ | 3175.4 | 0.0 | 3156.7 | 0.0 |

Continued on next page

TABLE IV – continued from previous page

| mode | sym. | B97-1/6-31g* freq. | B97-1/6-31g* int. | B97-1/TZ2P freq. | B97-1/TZ2P int. |
|---|---|---|---|---|---|
| $\nu_{20}$ | $B_{1u}$ | 1585.9 | 0.0 | 1577.7 | 0.0 |
| $\nu_{21}$ | $B_{1u}$ | 1453.2 | 0.0 | 1443.1 | 0.0 |
| $\nu_{22}$ | $B_{1u}$ | 1175.1 | 0.0 | 1181.5 | 0.0 |
| $\nu_{23}$ | $B_{1u}$ | 678.2 | 0.0 | 677.2 | 0.0 |
| $\nu_{24}$ | $B_{1u}$ | 560.0 | 0.0 | 563.3 | 0.0 |
| $\nu_{25}$ | $B_{2g}$ | 972.3 | 0.0 | 985.4 | 0.0 |
| $\nu_{26}$ | $B_{2g}$ | 789.7 | 0.0 | 869.0 | 0.0 |
| $\nu_{27}$ | $B_{2g}$ | 635.7 | 0.0 | 656.5 | 0.0 |
| $\nu_{28}$ | $B_{2g}$ | 227.8 | 0.0 | 224.1 | 0.0 |
| $\nu_{29}$ | $B_{2u}$ | 3190.7 | 0.0 | 3171.4 | 0.0 |
| $\nu_{30}$ | $B_{2u}$ | 1527.8 | 0.0 | 1511.2 | 0.0 |
| $\nu_{31}$ | $B_{2u}$ | 1381.8 | 0.0 | 1367.2 | 0.0 |
| $\nu_{32}$ | $B_{2u}$ | 1218.5 | 0.0 | 1205.0 | 0.0 |
| $\nu_{33}$ | $B_{2u}$ | 1168.5 | 0.0 | 1153.5 | 0.0 |
| $\nu_{34}$ | $B_{2u}$ | 476.9 | 0.0 | 477.0 | 0.0 |
| $\nu_{35}$ | $E_{1g}$ | 954.2 | 0.0 | 971.3 | 0.0 |
| $\nu_{36}$ | $E_{1g}$ | 954.2 | 0.0 | 971.3 | 0.0 |
| $\nu_{37}$ | $E_{1g}$ | 852.9 | 0.0 | 854.8 | 0.0 |
| $\nu_{38}$ | $E_{1g}$ | 852.9 | 0.0 | 854.8 | 0.0 |
| $\nu_{39}$ | $E_{1g}$ | 668.5 | 0.0 | 672.8 | 0.0 |
| $\nu_{40}$ | $E_{1g}$ | 668.5 | 0.0 | 672.8 | 0.0 |
| $\nu_{41}$ | $E_{1g}$ | 454.3 | 0.0 | 454.3 | 0.0 |
| $\nu_{42}$ | $E_{1g}$ | 454.3 | 0.0 | 454.3 | 0.0 |
| $\nu_{43}$ | $E_{1g}$ | 300.1 | 0.0 | 292.8 | 0.0 |
| $\nu_{44}$ | $E_{1g}$ | 300.1 | 0.0 | 292.8 | 0.0 |
| $\nu_{45}$ | $E_{1u}$ | 3193.0 | 107.828 | 3173.4 | 63.965 |
| $\nu_{46}$ | $E_{1u}$ | 3193.0 | 107.849 | 3173.4 | 63.973 |
| $\nu_{47}$ | $E_{1u}$ | 3173.6 | 6.729 | 3154.9 | 3.395 |
| $\nu_{48}$ | $E_{1u}$ | 3173.6 | 6.728 | 3154.9 | 3.406 |
| $\nu_{49}$ | $E_{1u}$ | 1660.5 | 12.129 | 1643.9 | 7.615 |
| $\nu_{50}$ | $E_{1u}$ | 1660.5 | 12.136 | 1643.9 | 7.623 |
| $\nu_{51}$ | $E_{1u}$ | 1540.8 | 1.630 | 1526.2 | 3.024 |
| $\nu_{52}$ | $E_{1u}$ | 1540.8 | 1.630 | 1526.2 | 3.026 |
| $\nu_{53}$ | $E_{1u}$ | 1435.1 | 0.815 | 1419.0 | 0.387 |
| $\nu_{54}$ | $E_{1u}$ | 1435.1 | 0.815 | 1419.0 | 0.392 |
| $\nu_{55}$ | $E_{1u}$ | 1339.0 | 23.446 | 1333.4 | 21.148 |
| $\nu_{56}$ | $E_{1u}$ | 1339.0 | 23.448 | 1333.4 | 21.126 |
| $\nu_{57}$ | $E_{1u}$ | 1241.4 | 1.029 | 1232.7 | 1.255 |
| $\nu_{58}$ | $E_{1u}$ | 1241.4 | 1.028 | 1232.7 | 1.254 |
| $\nu_{59}$ | $E_{1u}$ | 1161.6 | 7.599 | 1155.0 | 8.633 |
| $\nu_{60}$ | $E_{1u}$ | 1161.6 | 7.603 | 1155.0 | 8.628 |
| $\nu_{61}$ | $E_{1u}$ | 821.0 | 0.043 | 819.7 | 0.0014 |
| $\nu_{62}$ | $E_{1u}$ | 821.0 | 0.043 | 819.7 | 0.0012 |
| $\nu_{63}$ | $E_{1u}$ | 779.4 | 6.525 | 780.6 | 6.808 |
| $\nu_{64}$ | $E_{1u}$ | 779.4 | 6.525 | 780.6 | 6.797 |
| $\nu_{65}$ | $E_{1u}$ | 382.3 | 3.153 | 382.6 | 3.872 |
| $\nu_{66}$ | $E_{1u}$ | 382.3 | 3.153 | 382.6 | 3.867 |
| $\nu_{67}$ | $E_{2g}$ | 3191.5 | 0.0 | 3172.1 | 0.0 |
| $\nu_{68}$ | $E_{2g}$ | 3191.5 | 0.0 | 3172.1 | 0.0 |
| $\nu_{69}$ | $E_{2g}$ | 3174.8 | 0.0 | 3156.2 | 0.0 |
| $\nu_{70}$ | $E_{2g}$ | 3174.8 | 0.0 | 3156.2 | 0.0 |
| $\nu_{71}$ | $E_{2g}$ | 1660.0 | 0.0 | 1645.1 | 0.0 |
| $\nu_{72}$ | $E_{2g}$ | 1660.0 | 0.0 | 1645.1 | 0.0 |
| $\nu_{73}$ | $E_{2g}$ | 1487.9 | 0.0 | 1475.9 | 0.0 |

Continued on next page

TABLE IV – continued from previous page

| mode | sym. | B97-1/6-31g* freq. | B97-1/6-31g* int. | B97-1/TZ2P freq. | B97-1/TZ2P int. |
|---|---|---|---|---|---|
| $\nu_{74}$ | $E_{2g}$ | 1487.9 | 0.0 | 1475.9 | 0.0 |
| $\nu_{75}$ | $E_{2g}$ | 1470.6 | 0.0 | 1457.9 | 0.0 |
| $\nu_{76}$ | $E_{2g}$ | 1470.6 | 0.0 | 1457.9 | 0.0 |
| $\nu_{77}$ | $E_{2g}$ | 1430.8 | 0.0 | 1418.6 | 0.0 |
| $\nu_{78}$ | $E_{2g}$ | 1430.8 | 0.0 | 1418.6 | 0.0 |
| $\nu_{79}$ | $E_{2g}$ | 1254.5 | 0.0 | 1242.3 | 0.0 |
| $\nu_{80}$ | $E_{2g}$ | 1254.5 | 0.0 | 1242.3 | 0.0 |
| $\nu_{81}$ | $E_{2g}$ | 1187.1 | 0.0 | 1177.3 | 0.0 |
| $\nu_{82}$ | $E_{2g}$ | 1187.1 | 0.0 | 1177.3 | 0.0 |
| $\nu_{83}$ | $E_{2g}$ | 1006.6 | 0.0 | 1004.8 | 0.0 |
| $\nu_{84}$ | $E_{2g}$ | 1006.6 | 0.0 | 1004.8 | 0.0 |
| $\nu_{85}$ | $E_{2g}$ | 687.2 | 0.0 | 686.7 | 0.0 |
| $\nu_{86}$ | $E_{2g}$ | 687.2 | 0.0 | 686.7 | 0.0 |
| $\nu_{87}$ | $E_{2g}$ | 492.3 | 0.0 | 493.3 | 0.0 |
| $\nu_{88}$ | $E_{2g}$ | 492.3 | 0.0 | 493.3 | 0.0 |
| $\nu_{89}$ | $E_{2g}$ | 367.9 | 0.0 | 368.0 | 0.0 |
| $\nu_{90}$ | $E_{2g}$ | 367.9 | 0.0 | 368.0 | 0.0 |
| $\nu_{91}$ | $E_{2u}$ | 965.3 | 0.0 | 980.7 | 0.0 |
| $\nu_{92}$ | $E_{2u}$ | 965.3 | 0.0 | 980.7 | 0.0 |
| $\nu_{93}$ | $E_{2u}$ | 814.8 | 0.0 | 829.2 | 0.0 |
| $\nu_{94}$ | $E_{2u}$ | 814.8 | 0.0 | 829.2 | 0.0 |
| $\nu_{95}$ | $E_{2u}$ | 770.2 | 0.0 | 780.6 | 0.0 |
| $\nu_{96}$ | $E_{2u}$ | 770.2 | 0.0 | 780.6 | 0.0 |
| $\nu_{97}$ | $E_{2u}$ | 552.9 | 0.0 | 551.6 | 0.0 |
| $\nu_{98}$ | $E_{2u}$ | 552.9 | 0.0 | 551.6 | 0.0 |
| $\nu_{99}$ | $E_{2u}$ | 302.9 | 0.0 | 299.2 | 0.0 |
| $\nu_{100}$ | $E_{2u}$ | 302.9 | 0.0 | 299.2 | 0.0 |
| $\nu_{101}$ | $E_{2u}$ | 89.1 | 0.0 | 86.7 | 0.0 |
| $\nu_{102}$ | $E_{2u}$ | 89.1 | 0.0 | 86.7 | 0.0 |

It is well known that vibrational frequencies computed in the harmonic approximation can be brought in fairly good agreement with experimental values by scaling them with empirical scaling factors (see e. g. Ref. 5). The scaling factor(s) are typically obtained by fitting a large number of identified vibrational transitions, depend on the level of theory and basis set used, and may be different for different types of vibrations (i.e. stretches, bends, twists, the kinds of bonds involved etc.).[6,7] Scaling factors for the B97-1 functional in combination with the TZ2P basis set were obtained by Cané, Miani, and Trombetti[8] and confirmed by Maltseva *et al.*[9,10] with minimal variation. For the sake of comparison with anharmonic calculations we here used the original ones taken from Ref. 8, namely 0.9660 for C-H stretches and 0.982 for all the other bands. Given the very small sample of bands these factors were calibrated on, their general validity is not adequately tested, and they should be used with caution.

## III. ANHARMONIC BANDS OF PYRENE AS A FUNCTION OF $r$

The large set of bands listed in Table V results from anharmonic calculations with different $r$ values, keeping fixed $h = 8$. State assignment was done, as far as this table is concerned, on the calculation with $r = 0.3$, where it is the least ambiguous. In most eigenstates a single harmonic basis function is dominant. In the few cases where several harmonic basis functions have weights in the same range, the latter are all listed. Only transitions with non-negligible intensity are included in the table. When decreasing the $r$-value, some bands split in several ones due to resonances. Since this splitting may involve significant mixing with bands which are distinct at the $r = 0.3$ level, sometimes the same wave number appears several times in columns corresponding to smaller $r$ values. This happens, for example, for the bands which are computed at 3034, 3037, and 3042 $cm^{-1}$ at the $r = 0.3$ level. These give rise to a multitude of bands at smaller $r$ values, of which only the strongest are listed. Note also that, in some cases, distinct bands are almost coincident in position. However, they are listed on different lines in the table.

TABLE V: Calculated anharmonic band positions for pyrene as a function of the threshold $r$ and for fixed $h = 8$.

| mode | $r$=0.3 | $r$=0.2 | $r$=0.1 | $r$=0.05 |
|---|---|---|---|---|
| $\nu_{44}+\nu_{48}+\nu_{53}$, $\nu_5+\nu_{44}$ | 3144 | 3138, 3144, 3153 | 3134, 3144, 3146, 3154 | 3145, 3156 |
| $\nu_{44}+\nu_{57}$ | 3107 | 3105, 3106 | 3103, 3104 | 3098, 3102 |
| $\nu_{10}+\nu_{52}+\nu_{57}$ | 3102 | 3100 | 3099 | 3098, 3102 |
| $\nu_4+\nu_{45}$ | 3097 | 3097 | 3089, 3098 | 3092, 3098, 3102 |
| $\nu_{34}+\nu_{57}+\nu_{62}$ | 3096 | 3095 | 3092, 3093 | 3083, 3092, 3095 |
| $\nu_{26}+\nu_{57}$ | 3080 | 3079 | 3080 | 3062, 3073, 3078 |
| $\nu_{23}$ | 3055 | 3039, 3062, 3064, 3069 | 3010, 3029, 3035, 3069, 3104 | 3019, 3026, 3030, 3067, 3076 |
| $\nu_4+\nu_{28}$ | 3051 | 3023, 3030, 3036 | 3029, 3045, 3055, 3058 | 3056 |
| $\nu_{45}+\nu_{56}$ | 3043 | 3029, 3039, 3062, 3064, 3069 | 3029, 3035, 3045, 3055, 3069 | 3030, 3043, 3067, 3076 |
| $\nu_{42}$, $\nu_{43}$ | 3042 | 3042 | 3019, 3029, 3037, 3053 | 3023, 3040 |
| $\nu_4+\nu_{46}$ | 3037 | 3038 | 3029, 3037 | 3032, 3033, 3040, 3042, 3044, 3045 |
| $\nu_{43}$, $\nu_{42}$ | 3034 | 3035 | 2946, 3029, 3053 | 2940, 3032, 3033, 3044, 3045 |
| $\nu_{24}$ | 3031 | 3030 | 2954, 2969, 3010, 3045, 3078, 3079 | 2956, 3018, 3019, 3026, 3076 |
| $\nu_{49}+\nu_{61}$ | 2359 | 2359 | 2359 | 2359 |
| $\nu_{14}+\nu_{35}$ | 1936 | 1936 | 1937 | 1937 |
| $\nu_{35}+\nu_{66}$ | 1932 | 1932 | 1932 | 1934 |
| $\nu_{14}+\nu_{36}$ | 1922 | 1923 | 1919, 1937 | 1921, 1937 |
| $\nu_{36}+\nu_{66}$ | 1919 | 1919 | 1918 | 1919 |
| $\nu_{14}+\nu_{19}$ | 1866 | 1866 | 1865 | 1866 |
| $\nu_{15}+\nu_{35}$ | 1852 | 1552 | 1850 | 1848 |
| $\nu_{15}+\nu_{36}$ | 1839 | 1839 | 1838 | 1842 |
| $\nu_{35}+\nu_{67}$ | 1824 | 1825 | 1825 | 1823 |
| $\nu_{36}+\nu_{67}$ | 1809 | 1810 | 1810 | 1766, 1801, 1823 |
| $\nu_{37}+\nu_{66}$ | 1803 | 1803 | 1801, 1803 | 1801, 1809, 1810 |
| $\nu_{15}+\nu_{19}$ | 1790 | 1788 | 1790 | 1792 |
| $\nu_{14}+\nu_{20}$ | 1758 | 1761 | 1768 | 1766 |
| $\nu_{19}+\nu_{67}$ | 1745 | 1745 | 1745 | 1745 |
| $\nu_{17}+\nu_{18}+\nu_{35}+\nu_{71}$ | 1742 | 1742 | 1746 | 1741 |
| $\nu_{38}+\nu_{66}$ | 1740 | 1745 | 1746 | 1743 |
| $\nu_{15}+\nu_{37}$ | 1727 | 1727 | 1726 | 1726 |
| $\nu_{36}+\nu_{68}$, $\nu_{35}+\nu_{68}$ | 1705 | 1700 | 1701 | 1659, 1669, 1697 |
| $\nu_{15}+\nu_{20}$ | 1692 | 1692 | 1694 | 1659, 1669, 1697 |
| $\nu_{35}+\nu_{68}$, $\nu_{35}+\nu_{69}$, $\nu_{38}+\nu_{66}$ | 1687 | 1692 | 1684 | 1659, 1697, 1766 |
| $\nu_{36}+\nu_{69}$ | 1669 | 1665, 1668 | 1661, 1701 | 1659, 1669, 1697 |
| $\nu_{16}+\nu_{35}$ | 1655 | 1656 | 1655 | 1651 |

Continued on next page

TABLE V – continued from previous page

| mode | $r$=0.3 | $r$=0.2 | $r$=0.1 | $r$=0.05 |
|---|---|---|---|---|
| $\nu_{20}+\nu_{67}$ | 1646 | 1646 | 1645 | 1645 |
| $\nu_{16}+\nu_{36}$ | 1636 | 1637 | 1639 | 1636 |
| $\nu_{19}+\nu_{68}$ | 1617 | 1607, 1619 | 1606, 1618 | 1617 |
| $\nu_{38}+\nu_{67}$ | 1613 | 1613 | 1612 | 1612 |
| $\nu_{44}$ | 1597 | 1591, 1599 | 1592, 1598 | 1588, 1596, 1600 |
| $\nu_{53}+\nu_{60}$ | 1592 | 1592 | 1581, 1591 | 1590 |
| $\nu_{26}$ | 1585 | 1585 | 1586 | 1585 |
| $\nu_{16}+\nu_{19}$ $\nu_{17}+\nu_{53}+\nu_{67}$, $\nu_{53}+\nu_{60}$ | 1578 | 1578 | 1576, 1578 | 1575, 1578, 1581, 1585, 1590 |
| $\nu_{20}+\nu_{68}$ | 1544 | 1544 | 1544 | 1544 |
| $\nu_{39}+\nu_{66}$ | 1537 | 1540 | 1540 | 1537 |
| $\nu_{16}+\nu_{37}$ | 1521 | 1521 | 1521 | 1521 |
| $\nu_{20}+\nu_{69}$ | 1514 | 1514 | 1513 | 1510 |
| $\nu_{38}+\nu_{68}$ | 1509 | 1506 | 1509 | 1505 |
| $\nu_{21}+\nu_{66}$ | 1489 | 1489 | 1486 | 1485 |
| $\nu_{45}$ | 1475 | 1465, 1475 | 1461, 1463, 1474, 1486 | 1473 |
| $\nu_{14}+\nu_{40}$ $\nu_{51}+\nu_{64}$ | 1466 | 1464, 1465 | 1462, 1463 | 1447, 1453, 1459, 1460 |
| $\nu_{27}$ | 1444 | 1444 | 1442 | 1438, 1442, 1447 |
| $\nu_{28}$ | 1429 | 1417, 1425, 1429 | 1404, 1412, 1419, 1425, 1442 | 1424 |
| $\nu_{46}$ $\nu_{39}+\nu_{67}$ | 1419 | 1420 | 1414, 1418 | 1412, 1417 |
| $\nu_{51}+\nu_{65}$ | 1417 | 1411, 1417, 1429 | 1412, 1419, 1425, 1429 | 1409, 1418, 1424 |
| $\nu_{15}+\nu_{21}$ | 1412 | 1412 | 1410 | 1410 |
| $\nu_{47}$ | 1311 | 1311 | 1310 | 1311 |
| $\nu_{20}+\nu_{70}$ | 1286 | 1286 | 1286 | 1286 |
| $\nu_{21}+\nu_{68}$ | 1266 | 1266 | 1264 | 1264 |
| $\nu_{40}+\nu_{68}$ | 1243 | 1243 | 1242 | 1241 |
| $\nu_{29}$ | 1240 | 1240 | 1238 | 1236 |
| $\nu_{3}+\nu_{64}$ | 1190 | 1189 | 1189 | 1189 |
| $\nu_{49}$ | 1184 | 1184 | 1183 | 1179, 1180, 1181 |
| $\nu_{16}+\nu_{40}$ | 1181 | 1180 | 1180 | 1180, 1181 |
| $\nu_{17}+\nu_{38}$ | 1157 | 1157 | 1155 | 1153 |
| $\nu_{13}+\nu_{33}$ | 1096 | 1096 | 1097 | 1096 |
| $\nu_{30}$ | 1093 | 1093 | 1091 | 1089 |
| $\nu_{12}+\nu_{34}$ | 1084 | 1084 | 1081, 1082 | 1080, 1081 |
| $\nu_{53}+\nu_{63}$ | 1083 | 1083 | 1081, 1082 | 1080, 1081 |
| $\nu_{39}+\nu_{70}$ | 1059 | 1059 | 1058 | 1058 |
| $\nu_{52}+\nu_{65}$, $\nu_{31}$ | 999 | 997, 999 | 994, 995, 997 | 993, 996 |
| $\nu_{31}$, $\nu_{52}+\nu_{65}$ | 997 | 995, 997, 999 | 986, 994, 997 | 985, 993, 996 |
| $\nu_{66}$ | 962 | 962 | 962 | 962 |
| $\nu_{67}$ | 845 | 845 | 844 | 843 |
| $\nu_{32}$ | 820 | 820 | 817 | 816 |
| $\nu_{68}$ | 742 | 742 | 741 | 739 |
| $\nu_{69}$ | 712 | 712 | 711 | 710 |
| $\nu_{52}$ | 542 | 542 | 540 | 538 |
| $\nu_{34}$ | 497 | 497 | 495 | 493 |
| $\nu_{70}$ | 486 | 486 | 484 | 483 |
| $\nu_{53}$ | 349 | 349 | 349 | 342, 347 |
| $\nu_{71}$ | 202 | 202 | 200 | 199 |
| $\nu_{72}$ | 95 | 95 | 94 | 92 |

## IV. ANHARMONIC SPECTRA OF PYRENE AND CORONENE

In this section we provide, for reference and easier comparison with experimental and/or other theoretical spectra, complete plots of our best computed anharmonic spectra for Pyrene (from Fig. 1 to 13) and Coronene (from Fig. 14 to 27). Each figure covers a range of 300 $cm^{-1}$, and consecutive plots have an overlap of

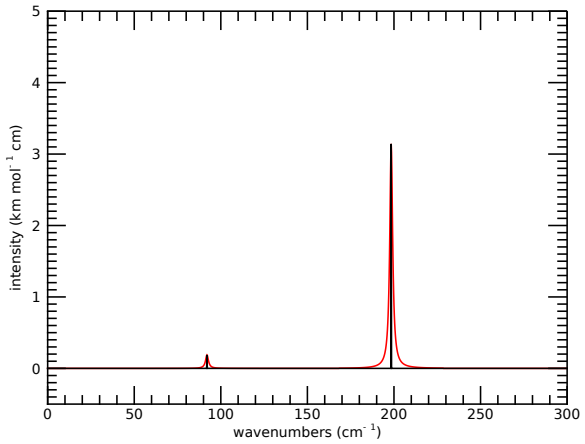


FIG. 1. Anharmonic spectrum of Pyrene computed with $r = 0.05$ and $h = 8$ in the range from 0 to 300 cm$^{-1}$. Black bars indicate the precise position of individual bands, whereas red envelopes are convolved with Lorentzian profiles with a 1 cm$^{-1}$ width.

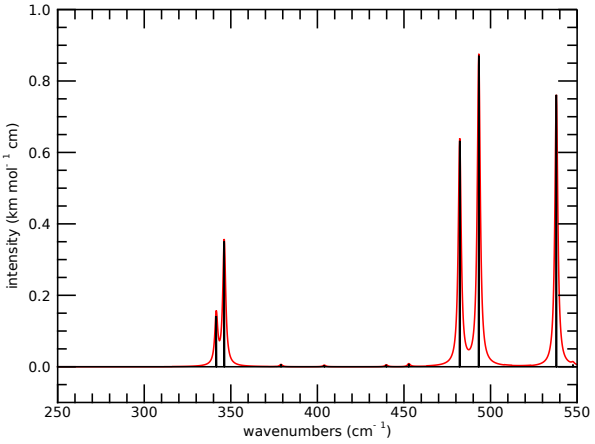


FIG. 2. Same as Fig. 1 in the range from 250 to 550 cm$^{-1}$.

50 cm$^{-1}$. The overall spectrum, in red, was obtained by convolving individual bands with a Lorentzian profile with a 1 cm$^{-1}$ width. Intensities of the convolved spectra are absolute and expressed in km mol$^{-1}$cm, the standard units of quantum chemistry calculations. The precise positions of individual bands are marked in the spectra by black bars. The complete, anharmonic, tabulated spectra of Pyrene and Coronene can be found in the online PAH database by Malloci, Joblin, and Mulas.[11]

[1]P. S. Thomas and T. C. Jr., J. Chem. Phys. **146**, 204110 (2017).
[2]D. Bégué, N. Gohaud, C. Pouchan, P. Cassam-Chenaï, and J. Liévin, J. Chem. Phys. **127**, 164115 (2007).
[3]P. S. Thomas and T. Carrington, J. Phys. Chem. A **119**, 13074 (2015).

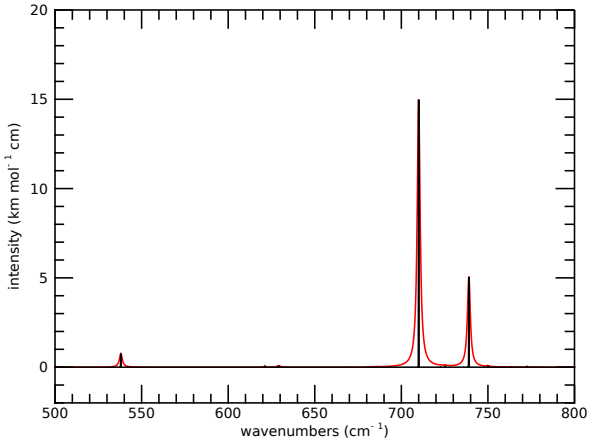


FIG. 3. Same as Fig. 1 in the range from 500 to 800 cm$^{-1}$.

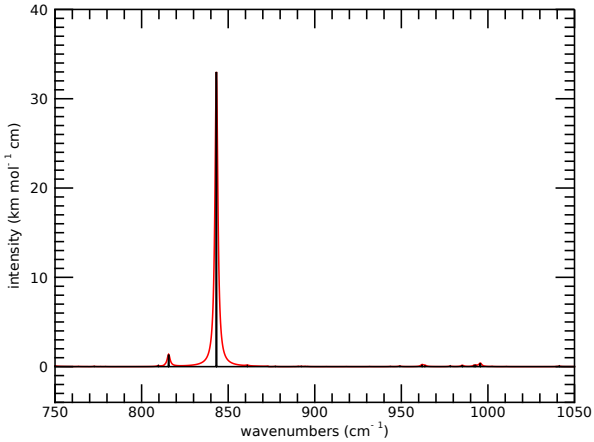


FIG. 4. Same as Fig. 1 in the range from 750 to 1050 cm$^{-1}$.

[4]M. Odunlami, V. L. Bris, D. Bégué, I. Baraille, and O. Coulaud, J. Chem. Phys. **146**, 214108 (2017).
[5]K. K. Irikura, R. D. Johnson, and R. N. Kacker, J. Phys. Chem. A **109**, 8430 (2005).
[6]F. Pauzat, D. Talbi, and Y. Ellinger, Astron. Astrophys. **293**, 263 (1995).
[7]F. Pauzat, D. Talbi, and Y. Ellinger, Astron. Astrophys. **319**, 318 (1997).
[8]E. Cané, A. Miani, and A. Trombetti, J. Phys. Chem. A **111**, 8218 (2007).
[9]E. Maltseva, A. Petrignani, A. Candian, C. J. Mackie, X. Huang, T. J. Lee, A. G. G. M. Tielens, J. Oomens, and W. J. Buma, Astrophys. J. **814**, 23 (2015).
[10]E. Maltseva, A. Petrignani, A. Candian, C. J. Mackie, X. Huang, T. J. Lee, A. G. G. M. Tielens, J. Oomens, and W. J. Buma, Astrophys. J. **831**, 58 (2016).
[11]G. Malloci, C. Joblin, and G. Mulas, Chem. Phys. **332**, 353 (2007), astro-ph/0701254.

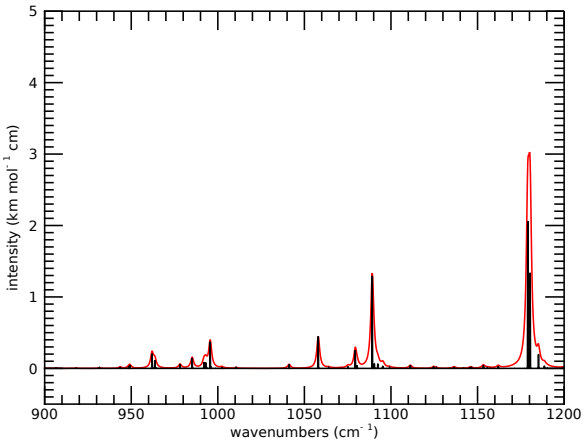


FIG. 5. Same as Fig. 1 in the range from 900 to 1200 cm$^{-1}$.

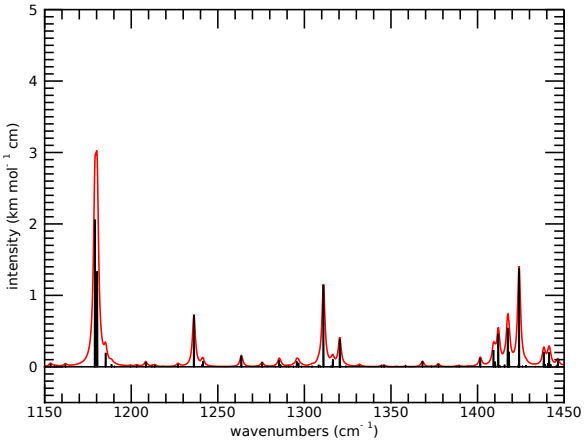


FIG. 6. Same as Fig. 1 in the range from 1150 to 1450 cm$^{-1}$.

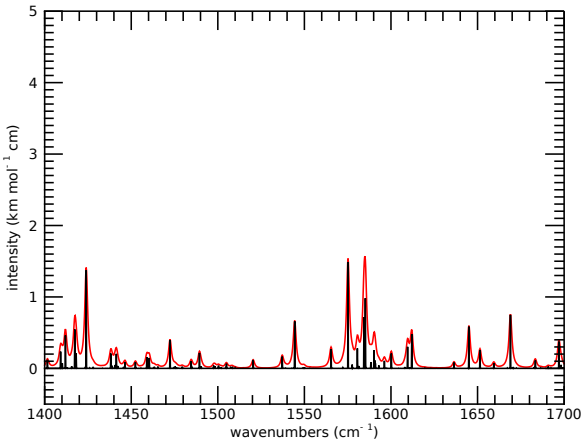


FIG. 7. Same as Fig. 1 in the range from 1400 to 1700 cm$^{-1}$.

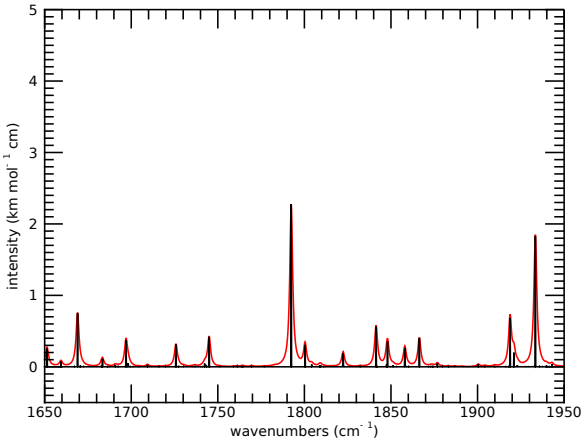


FIG. 8. Same as Fig. 1 in the range from 1650 to 1950 cm$^{-1}$.

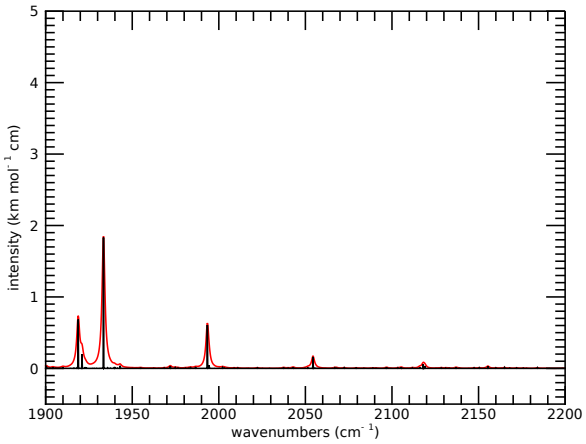


FIG. 9. Same as Fig. 1 in the range from 1900 to 2200 cm$^{-1}$.

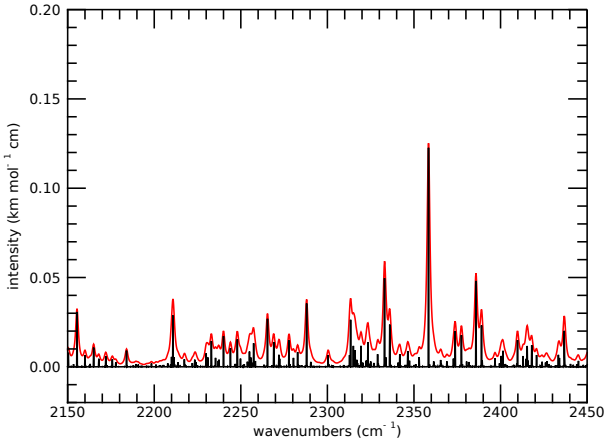


FIG. 10. Same as Fig. 1 in the range from 2150 to 2450 cm$^{-1}$.

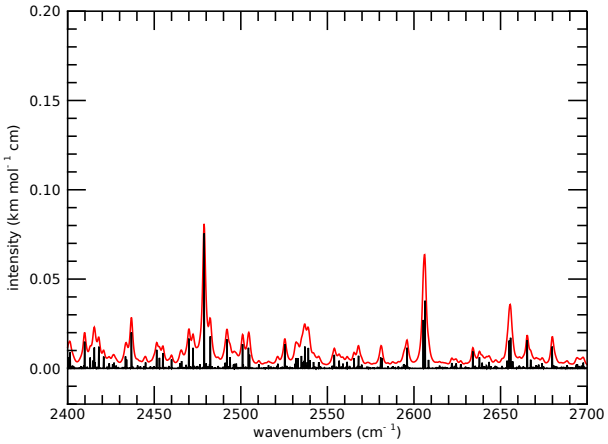


FIG. 11. Same as Fig. 1 in the range from 2400 to 2700 cm$^{-1}$.

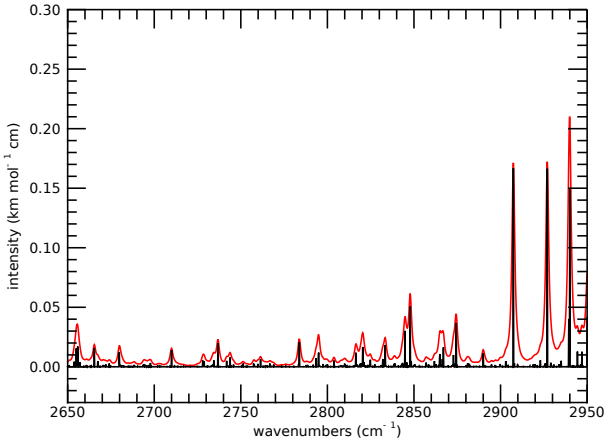


FIG. 12. Same as Fig. 1 in the range from 2650 to 2950 cm$^{-1}$.

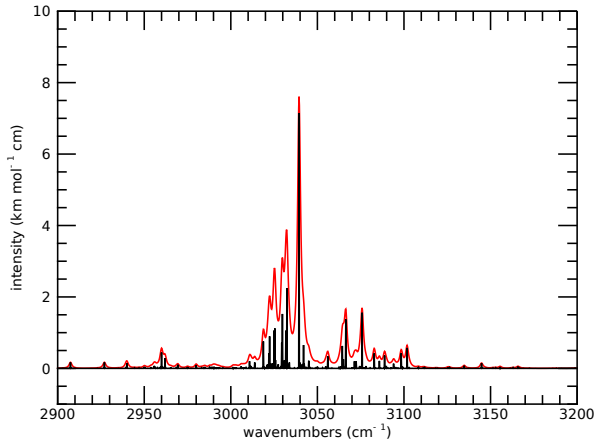


FIG. 13. Same as Fig. 1 in the range from 2900 to 3200 cm$^{-1}$.

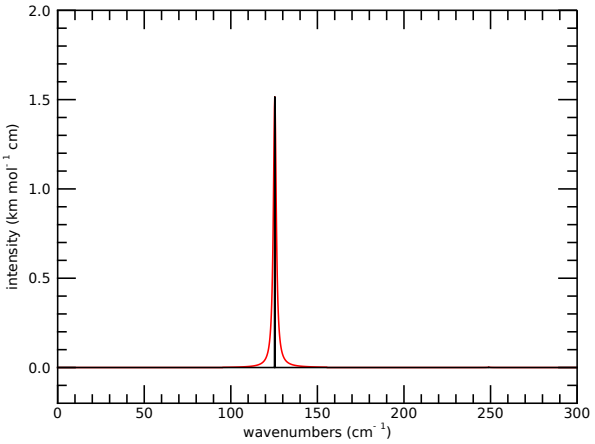


FIG. 14. Anharmonic spectrum of Coronene computed with $r = 0.1$ and $h = 6$ in the range from 0 to 300 cm$^{-1}$. Black bars indicate the precise position of individual bands, whereas red envelopes are convolved with Lorentzian profiles with a 1 cm$^{-1}$ width.

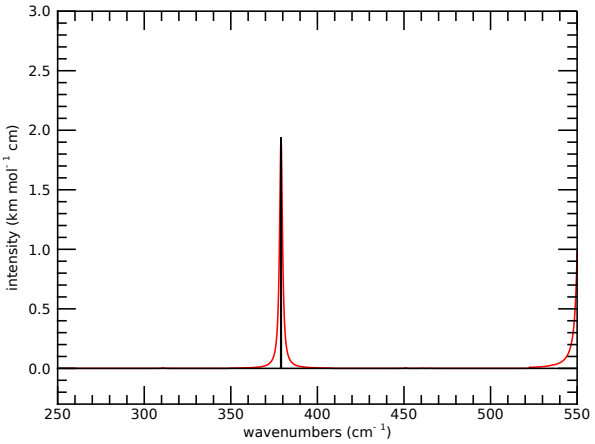


FIG. 15. Same as Fig. 14 in the range from 250 to 550 cm$^{-1}$.

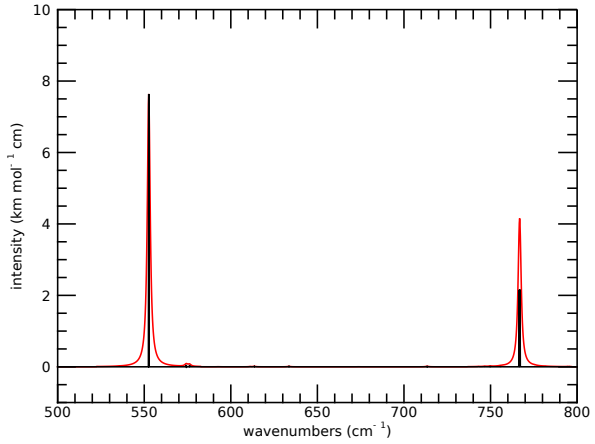


FIG. 16. Same as Fig. 14 in the range from 500 to 800 cm$^{-1}$.

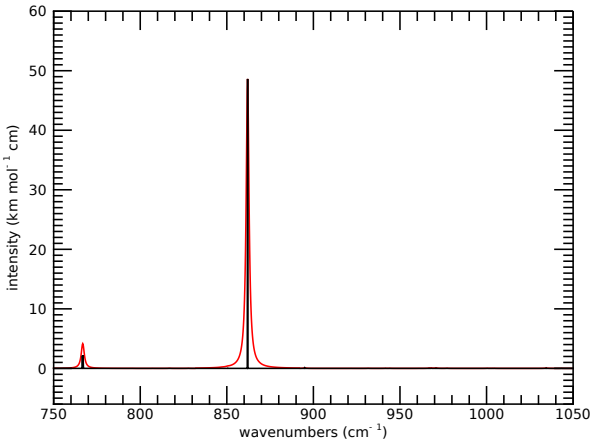


FIG. 17. Same as Fig. 14 in the range from 750 to 1050 cm$^{-1}$.

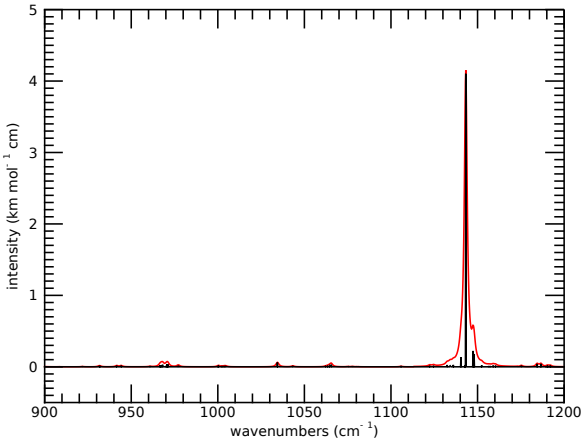


FIG. 18. Same as Fig. 14 in the range from 900 to 1200 cm$^{-1}$.

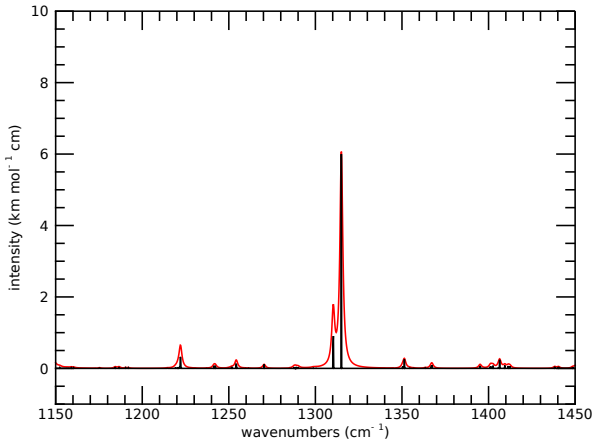


FIG. 19. Same as Fig. 14 in the range from 1150 to 1450 $cm^{-1}$.

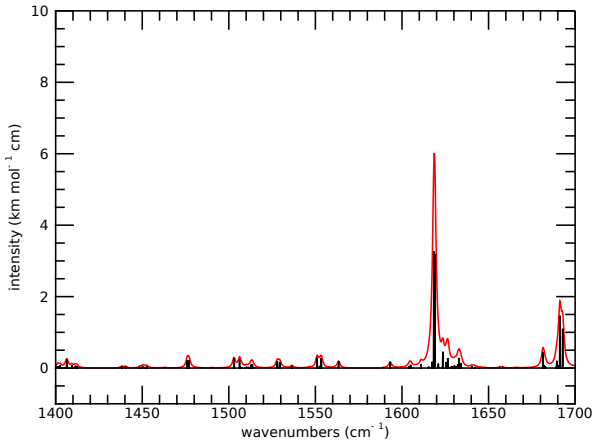


FIG. 20. Same as Fig. 14 in the range from 1400 to 1700 $cm^{-1}$.

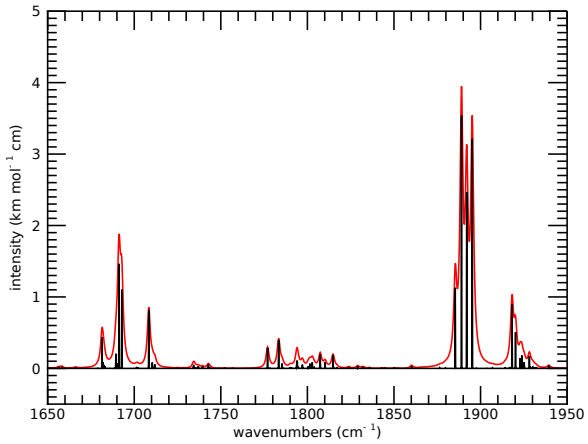


FIG. 21. Same as Fig. 14 in the range from 1650 to 1950 $cm^{-1}$.

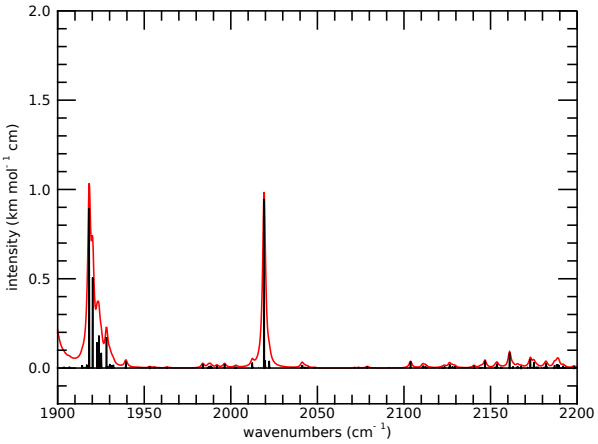


FIG. 22. Same as Fig. 14 in the range from 1900 to 2200 $cm^{-1}$.

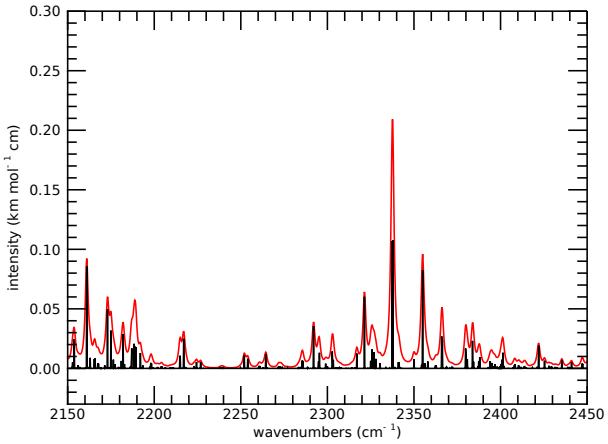


FIG. 23. Same as Fig. 14 in the range from 2150 to 2450 $cm^{-1}$.

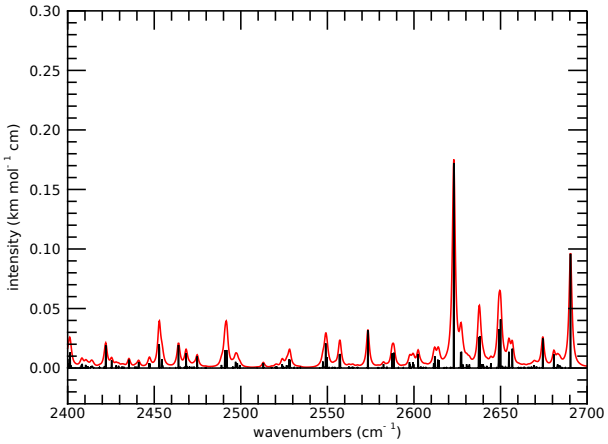


FIG. 24. Same as Fig. 14 in the range from 2400 to 2700 $cm^{-1}$.

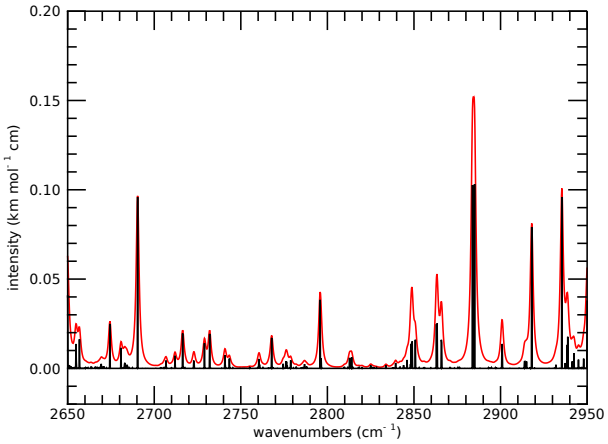


FIG. 25. Same as Fig. 14 in the range from 2650 to 2950 $cm^{-1}$.

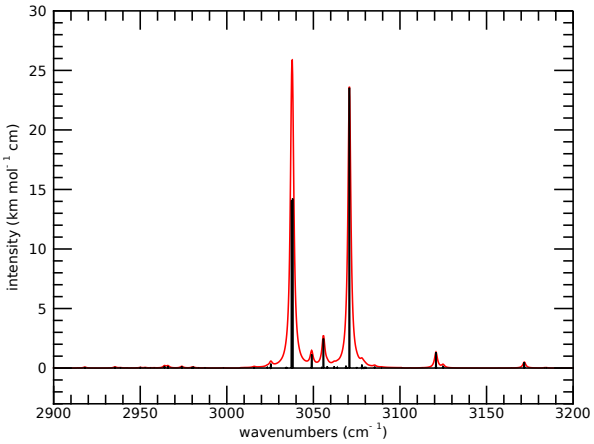


FIG. 26. Same as Fig. 14 in the range from 2900 to 3200 $cm^{-1}$.

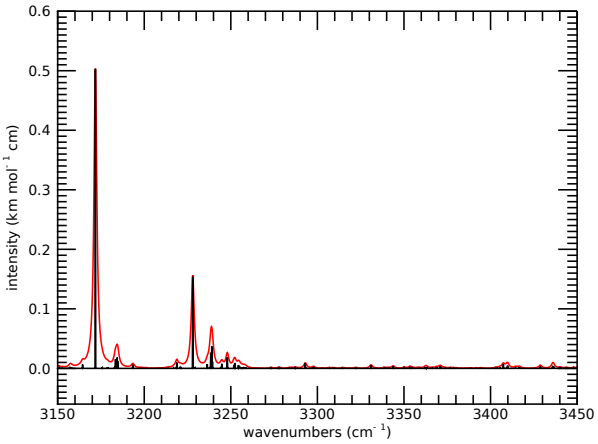


FIG. 27. Same as Fig. 14 in the range from 3150 to 3450 $cm^{-1}$.